Bed nucleus of the stria terminalis mediates fear to ambiguous threat signals

Travis D. Goode[1], Reed L. Ressler[1], Gillian M. Acca[1], Stephen Maren[1,2]

[1]*Department of Psychological and Brain Sciences and Institute for Neuroscience, Texas A&M University, College Station, TX, 77843-3474, USA*

[2]*Corresponding author*

Email:	maren@tamu.edu
Phone:	979-458-7960
Address:	Stephen Maren Department of Psychological and Brain Sciences Texas A&M University 301 Old Main Dr. College Station, TX 77843-3474

ORCiD

Travis D. Goode:	https://orcid.org/0000-0003-1432-8894
Reed L. Ressler:	https://orcid.org/0000-0003-0514-8269
Stephen Maren:	https://orcid.org/0000-0002-9342-7411

ABSTRACT

The bed nucleus of the stria terminalis (BNST) has been implicated in fear and anxiety, but the specific factors that engage the BNST in defensive behavior are unclear. Here we explore the possibility that ambiguous threats recruit the BNST during Pavlovian fear conditioning in rats. We arranged a conditioned stimulus (CS) to either precede or follow an aversive unconditioned stimulus (US), a procedure that established reliable (forward) or ambiguous (backward) signals for US onset. After conditioning, reversible inactivation of the BNST selectively reduced freezing to the backward CS; BNST inactivation did not affect freezing to the forward CS even when that CS predicted a variable magnitude US. Backward CSs increased Fos in the ventral BNST and in BNST-projecting neurons in the infralimbic cortex, but not the hippocampus or amygdala. These data reveal that BNST circuits process ambiguous threat signals central to the etiology and expression of anxiety.

INTRODUCTION

Excessive apprehension about potential future threats, including financial loss, illness, or death, is a defining feature of many anxiety disorders, including generalized anxiety disorder (GAD). Anxiety and trauma-related disorders are widespread and costly (Blanco et al., 2011; Comer et al., 2011; Kinley et al., 2011; Salas-Wright et al., 2014; Stein et al., 2017; Wittchen, 2002), and remain difficult to treat (Colvonen et al., 2017; Costello et al., 2014; Iza et al., 2013; Sinnema et al., 2015). Understanding the neural circuits underlying anxiety is important for refining behavioral and pharmacotherapeutic treatments (Deslauriers et al., 2017; Fanselow and Pennington, 2018, 2017; Graham et al., 2014; LeDoux and Daw, 2018; Nees et al., 2015; Pine and LeDoux, 2017). Several recent studies have demonstrated changes in the activity of the bed nucleus of the stria terminalis (BNST) in individuals with anxiety disorders (Brinkmann et al., 2018, 2017; Buff et al., 2017; Rabellino et al., 2018). However, the conditions that recruit the BNST to aversive learning and memory processes believed to underlie anxiety disorders are still not understood (Avery et al., 2016; Ch'ng et al., 2018; Fox and Shackman, 2017; Goode and Maren, 2017; Gungor and Paré, 2016; Lebow and Chen, 2016; Perusini and Fanselow, 2015; Shackman and Fox, 2016).

Early work on this question revealed that BNST lesions in rats impair defensive behaviors evoked by unconditioned threats (Gewirtz et al., 1998). For example, unconditioned increases in the acoustic startle reflex produced by either intracranial administration of corticotropin releasing factor (CRF) or exposure to bright light require the BNST, whereas fear-potentiated startle to punctate conditioned stimuli (CSs) do not (Walker et al., 2009). However, the involvement of the BNST in defensive responding is not restricted to unconditioned threat: BNST lesions produce deficits in both freezing and corticosterone release elicited by contextual, but not auditory, CSs

after Pavlovian fear conditioning in rats (LeDoux et al., 1988; Sullivan et al., 2004). Interestingly, however, it is not stimulus modality that differentiates the effects of BNST lesions on tone and context freezing. BNST lesions impair freezing responses to long-duration (e.g., 10-min) auditory conditioned stimuli (CSs) (Waddell et al., 2006), and spare freezing to short-duration (1-min) contextual stimuli (Hammack et al., 2015). Based on this work, it has been proposed that the BNST is required to organize behavioral and hormonal responses to sustained threats (whether conditioned or unconditioned) (Hammack et al., 2015, 2009; Takahashi, 2014; Waddell et al., 2008, 2006). Of course, the duration of the behavioral responses in these situations is confounded with the duration of the eliciting stimulus. Thus, it has been argued that the BNST mediates sustained defensive *responses* independent of the specific features and durations of the stimuli that evoke them (Davis, 2006; Davis et al., 2010; Walker and Davis, 2008; Walker et al., 2009).

Of course, another factor that differentiates discrete tones from contexts, or short- from long-duration stimuli (whether tones or contexts), is the temporal information the stimuli provide about when an aversive event will occur (Goode and Maren, 2017). For example, long-duration CSs or contexts provide relatively poor information about when a future US will occur (i.e., the US will occur sometime in the future), whereas short-duration CSs or contexts provide more certainty about US onset (i.e., the US will occur soon). We and others have proposed that the BNST may have a critical role in processing temporally ambiguous threats, particularly stimuli that poorly predict when an aversive event will occur (Goode and Maren, 2017; Lange et al., 2017). Consistent with this view, punctate auditory CSs that are followed by shock at unpredictable latencies yield freezing responses that are sensitive to BNST manipulations (Daldrup et al., 2016; Lange et al., 2017). This suggests that a crucial parameter that determines the role for the BNST in defensive behavior is neither the duration nor modality of the threat (nor the duration of the

elicited defensive response), but rather the information a signal provides about when an aversive event will occur.

Here we examined this possibility by examining the role of the BNST in conditioned freezing elicited by procedures that equated both the duration and modality of the threat CSs, but differed according to the timing of the aversive unconditioned stimulus (US) in relation to the CS. Specifically, we arranged a brief (10-sec) auditory CS to either precede (forward conditioning, FW) or follow (backward conditioning, BW) a footshock US in rats; this design resulted in CSs that were either poor (BW) or good (FW) predictors of when the US would occur. We hypothesized that pharmacological inactivation of the BNST would selectively disrupt fear expression to the BW CS, and that BW CSs would produce activity in greater numbers of BNST neurons than the FW CS. Furthermore, we anticipated that the backward CS would increase the activity of BNST-projecting neurons in afferent brain regions implicated in anxiety states.

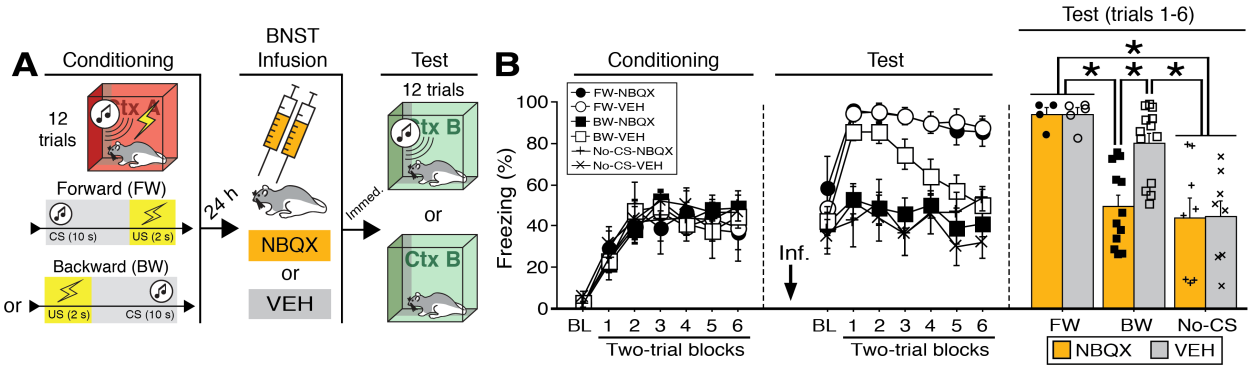

Figure 1. *Reversible inactivation of the BNST attenuates conditioned fear expression to a backward, but not forward, CS.* **(A)** Behavioral schematic. **(B)** Freezing behavior during at conditioning and retrieval testing. For conditioning, the left panel depicts mean percentage freezing during the 5-min baseline (BL) and across each conditioning block (each block is comprised of two trials; conditioning trials consist of freezing during the 10-sec CS followed by the 58-sec interval). For retrieval testing, the center panel shows mean percentage freezing at the 5-min baseline (BL) and across each test block (each block is comprised of two trials; trials consist of freezing during the 10-sec CS followed by the 60-sec interval). The right panel shows mean percentage freezing during the first half of the test (trials 1-6). All data are represented as means ± s.e.m [FW-NBQX (n = 4); FW-VEH (n = 5); BW-NBQX (n = 12); BW-VEH (n = 13); No-CS-NBQX (n = 8), No-CS-VEH (n = 8)]; * = $p < 0.05$.

RESULTS

Reversible inactivation of the BNST attenuates fear to a backward, but not forward, CS. To examine the role of the BNST in threat uncertainty, we reversibly inactivated the BNST during retrieval of fear to either a forward- ("FW"; certain threat) or backward-trained ("BW"; uncertain threat) CS. A schematic of the behavioral design is shown in Figure 1A. Representative cannula tracts and histological placements are presented in Figure 1—Figure Supplement 1 and Figure 1—Figure Supplement 2A (respectively). Freezing behavior during the conditioning session is shown in Figure 1B. A main effect of conditioning trial was observed (repeated measures ANOVA: $F_{6,288} = 37.87$, $p < 0.0001$). No significant main effects or interactions were observed for any of the conditioning or drug assignments across the conditioning trials (ANOVA: F's < 0.70, p's > 0.60).

One day after conditioning, the animals were infused with NBQX, an AMPA receptor antagonist, to reversibly inactivate the BNST; saline ("VEH") infusions served as a control. Immediately after the infusions, the rats were placed in a novel context and received twelve presentations of the CS (some BW-trained rats received no CS exposure, "No-CS"). As shown in (Figure 1B), inactivation of the BNST produced a selective decrease in conditioned freezing to the BW CS. Analysis of freezing behavior across the entire session (including the baseline) revealed a main effect of trial (repeated measures: $F_{6,264} = 8.06$, $p < 0.0001$), a significant main effect of CS exposure ($F_{2,44} = 25.38$, $p < 0.0001$), and a significant CS × drug interaction ($F_{2,44} = 3.66$, $p < 0.05$). There were no other main effects or interactions (ANOVA: F's < 1.6, p's > 0.05). Fisher's PLSD indicated that rats in the FW condition exhibited significantly more freezing during the retrieval test than rats in all other groups (p's < 0.05). Importantly, BW-VEH rats exhibited

81 significantly higher levels of freezing than BW-VEH rats ($p < 0.005$), which did not differ from
82 the No-CS groups.

83 Given that freezing to the BW CS in the VEH-treated animals was maximal in the first half
84 of the test, a separate factorial ANOVA was performed on the average percentage of freezing
85 during trials 1-6 (Figure 1B). For this period, there was a main effect of CS ($F_{2,44} = 18.61$, $p <$
86 0.0001) as well as a CS × drug interaction ($F_{2,44} = 3.81$, $p < 0.05$); there was no main effect of drug
87 ($F < 3.00$, $p > 0.05$). Fisher's PLSD revealed significant differences in NBQX- and VEH-treated
88 animals in both the BW and FW groups (p's < 0.0005). Additionally, rats in the No-CS groups
89 differed from all others (p's < 0.0005) except those in the BW-NBQX group. It has been suggested
90 that the BNST mediates sustained but not acute fear responses (Davis, 2006; Davis et al., 2010;
91 Walker and Davis, 2008; Walker et al., 2009). However, it is notable that in this experiment BNST
92 inactivation selectively attenuated conditioned freezing to the backward CS, which produced less
93 sustained freezing during the retrieval test compared to the FW CS.

94 The different effects of BNST inactivation on freezing to FW and BW CSs may have been
95 related to differences in memory strength between the two CSs (reflected in overall levels of
96 freezing to each CS across the retrieval test). Indeed, to generate conditioned freezing to a
97 backward CS we used more conditioning trials than typical in our experiments. This of course
98 resulted in moderate overtraining of the forward CS, which might have rendered the FW response
99 less sensitive to disruption. To examine this possibility, we examined the effects of BNST
100 inactivation of FW and BW conditioning established with five conditioning trials (Figure 2). The
101 behavioral design for the five-trial experiment is shown in Figure 2A; cannula placements are
102 shown in Figure 2—Figure Supplement 1.

103 During the 5-trial conditioning procedure (Figure 2B), animals exhibited reliable increases
104 in freezing across the session (repeated measures ANOVA: $F_{5,115} = 12.154$, $p < 0.0001$; there were
105 no main effects of conditioning procedure or drug treatment and no interaction of these variables:
106 F's < 2.3, p's > 0.15). After infusions of NBQX or VEH, animals were tested to the CS in a familiar
107 context that was distinct from the conditioning context. As shown in Figure 2B, BNST inactivation
108 did not affect conditioned freezing to either the FW or BW CS. An ANOVA revealed a main effect
109 of trial (repeated measures [including baseline freezing]: $F_{5,105} = 22.118$, $p < 0.0001$), a main effect
110 of conditioning procedure ($F_{1,21} = 15.930$, $p < 0.001$), and a trial × conditioning procedure
111 interaction (repeated measures: $F_{5,105} = 12.346$, $p < 0.0001$). A separate ANOVA performed on
112 trials 1-5 (excluding baseline; Figure 2B) revealed a significant main effect of conditioning
113 procedure ($F_{1,21} = 21.585$, $p = 0.0001$; there was no main effect of drug and no interaction: F's <
114 0.15, p's > 0.7). Thus, the failure of BNST inactivation to impair conditioned freezing to the FW
115 CS in the 12-trial procedure was not due to a ceiling effect; freezing to the FW CS in the 5-trial
116 procedure was relatively lower and remained insensitive to BNST inactivation. The absence of an
117 effect of BNST inactivation on freezing to the BW CS in this experiment is likely due to a floor
118 effect insofar as the 5-trial procedure did not yield conditional freezing to the CS (at least freezing
119 that exceeded the pre-CS baseline). Together, these data indicate that the BNST is required for the
120 expression of conditioned freezing to a BW, but not FW, CS.

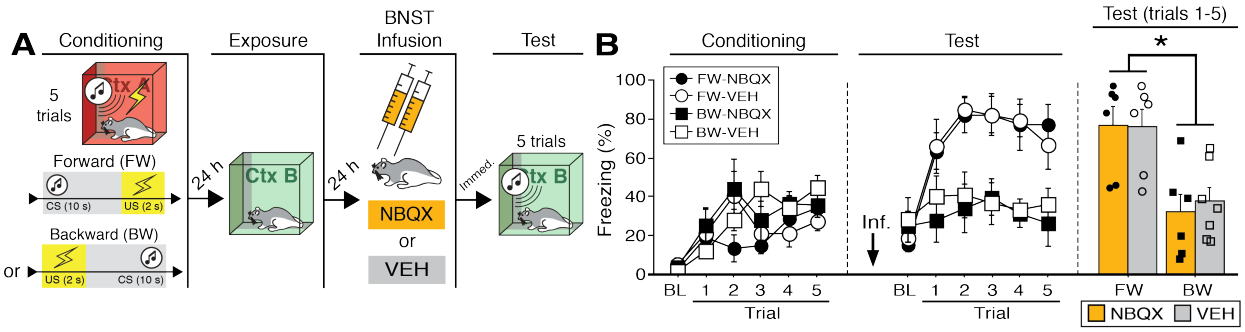

Figure 2. *Effects of BNST inactivation on freezing to a forward vs. backward CS trained with five trials.* **(A)** Behavioral schematic. **(B)** Freezing behavior during conditioning and retrieval testing. For conditioning, the left panel depicts mean percentage freezing during the 3-min baseline (BL) and across each conditioning block (each block is comprised of two trials; conditioning trials consist of freezing during the 10-sec CS followed by the 58-sec interval). For retrieval testing, the center panel shows mean percentage freezing at the 3-min baseline (BL) and across each test block (each block is comprised of two trials; trials consist of freezing during the 10-sec CS followed by the 60-sec interval). The right panel shows mean percentage freezing after baseline (trials 1-5). All data are represented as means ± s.e.m [FW-NBQX (n = 6); FW-VEH (n = 6); BW-NBQX (n = 6); BW-VEH (n = 7)]; * = $p < 0.05$.

The differential effect of BNST inactivation on freezing to a FW or BW CS suggests that the BNST regulates defensive behavior to stimuli that poorly signal US onset. One index that might reveal differences in the ability of the CS to predict the US is the US-evoked response itself. Footshock USs elicit an unconditioned response (UR) that includes vocalization, autonomic adjustments, and burst of locomotor activity (Bali and Jaggi, 2015; Fanselow, 1994). To better understand the mechanisms of forward and backward conditioning on behavior, we examined shock-evoked activity bursts (Kunwar et al., 2015; Zelikowsky et al., 2018) during the conditioning session in a separate cohort of animals (a separate cohort was analyzed in order to compare equal numbers of FW- and BW-conditioned animals) (Figure 3). Fear conditioning resulted in robust freezing in both groups of animals (Figure 3A). An ANOVA revealed a significant main effect of trial ($F_{6,180} = 67.02$, $p < 0.0001$) with no differences between levels of freezing in FW or BW animals (no other main effect and no interaction: F's < 1.80, p's > 0.15). In contrast, shock-induced activity differed in FW and BW animals (Figure 3C). All animals

134 exhibited a reliable decrease in shock-induced activity across the conditioning session ($F_{5,150}$ =
135 9.59, $p < 0.0001$) and the rate of decline in activity was similar in the two groups (no trial × group
136 interaction: $F < 1.70$, $p > 0.09$), but the overall level of shock-induced activity was significantly
137 higher in BW animals (main effect of group: $F_{1,30} = 9.59$, $p < 0.05$). For comparison, two-tailed
138 unpaired *t*-test of mean levels of activity during the 5-min baseline revealed no significant
139 difference between FW and BW rats (Figure 3B; $t < 0.30$; $p > 0.75$). Hence, USs that were not
140 signaled by a forward CS evoked greater activity bursts than those that were. Collectively, these
141 data suggest that temporal uncertainty is an important factor in recruiting the BNST to fear.

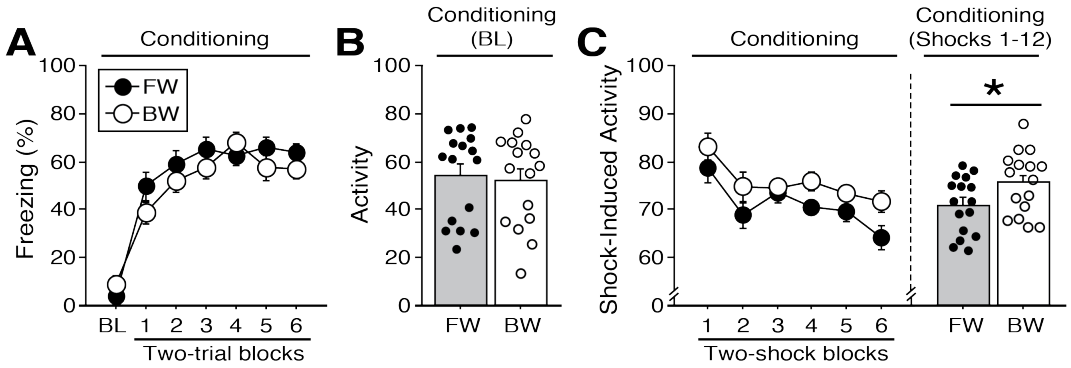

Figure 3. *Shock-induced activity during conditioning to a forward vs. backward CS.* **(A)** Mean percentage of freezing at baseline (BL; 5-min) and across conditioning blocks (each block is comprised of two trials; trials consist of freezing during the 10-sec CS followed by the 58-sec interval). **(B)** Mean activity values across the 5-min BL (no shock present). **(C)** The left panel shows mean shock-induced activity during conditioning (averaged into two-shock blocks). The right panel shows mean shock-induced activity across all trials. All data are represented as means ± s.e.m [FW (n = 16); BW (n = 16)]; * = $p < 0.05$.

142 ***Temporary inactivation of the BNST does not eliminate fear to a forward CS that is paired with***
143 ***a US of variable intensity.*** To determine whether the BNST is involved in other conditioning
144 procedures imbued with outcome uncertainty, we examined whether freezing to a FW CS that is
145 paired with a US of variable intensity is also BNST-dependent. In this case, rats received forward
146 fear conditioning with either a fixed ("FIXED") or variable ("VARIABLE") US intensity (Figure

147 4). A schematic of the behavioral design is shown in Figure 4A; cannula placements are illustrated

148 in Figure 4—Figure Supplement 1. During conditioning (Figure 4B), a repeated measures

149 ANOVA revealed a main effect of trial ($F_{6,168} = 68.15$, $p < 0.0001$), with no main effect of drug or

150 conditioning procedure, and no interactions (F's < 1.50, p's > 0.20).

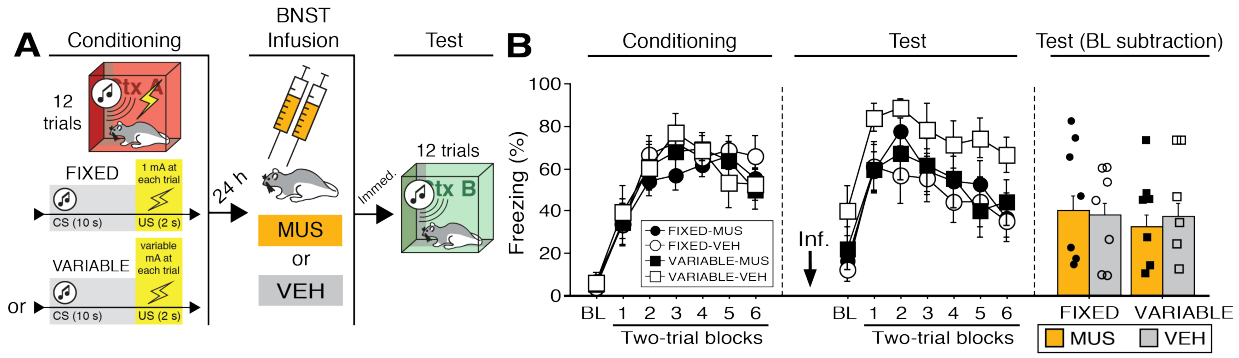

Figure 4. *Temporary inactivation of the BNST does not prevent conditioned fear expression to a forward CS paired with a US of fixed or variable intensity.* **(A)** Behavioral schematic. **(B)** Freezing behavior during conditioning and retrieval testing. For conditioning, the left panel depicts mean percentage freezing during the 5-min baseline (BL) and across each conditioning block (each block is comprised of two trials; trials consist of freezing during the 10-sec CS followed by the 58-sec interval). For retrieval testing, the center panel shows mean percentage freezing at the 5-min baseline (BL) and across each test block (each block is comprised of two trials; trials consist of freezing during the 10-sec CS followed by the 60-sec interval). The right panel shows mean percentage freezing across all test trials (after BL), with BL levels of freezing subtracted from these values. All data are represented as means ± s.e.m [FIXED-MUS (n = 8); FIXED-VEH (n = 7); VARIABLE-MUS (n = 8); VARIABLE-VEH (n = 7)].

151 Twenty-four hours after conditioning and immediately before a test to the CS in a novel

152 context (Figure 4B), the animals were infused with either muscimol ("MUS") to reversibly

153 inactivate the BNST; saline ("VEH") infusions served as a control. As shown in Figure 4B, BNST

154 inactivation did not affect freezing to a FW CS paired with either a fixed or variable US. During

155 retrieval testing, there was a main effect of trial ($F_{6,156} = 24.31$, $p < 0.0001$), however no other

156 main effects or interactions were detected (F's < 2.70, p's > 0.15). Although average baseline

157 freezing was highest in VARIABLE-VEH animals, an ANOVA of baseline freezing did not reveal

158 any main effects or interactions (F's < 3.60, p's > 0.05). To equate for differences in pre-CS

159 freezing in the experimental groups, baseline freezing was subtracted from CS-elicited freezing
160 (Figure 4B). This did not reveal an effect of BNST inactivation on freezing; there were no
161 significant main effects or interactions in the ANOVA (F's < 0.15, p's > 0.70). Although BNST
162 inactivation tended to reduce generalized contextual freezing, it did not significantly impact
163 freezing to the temporally predictable CS, regardless of US intensity.
164
165 ***Backward CSs selectively increase Fos expression in the ventral BNST.*** To further examine the
166 role of the BNST in the expression of fear to a BW CS, we quantified Fos expression in multiple
167 subregions of the BNST following the presentation of either a FW or BW CS during a shock-free
168 retrieval test (Figure 5). The behavioral design is summarized in Figure 5A. Four experimental
169 groups were compared: rats conditioned and tested to a forward CS ("FW"), rats conditioned and
170 tested to a backward CS ("BW"), rats conditioned to a forward or backward CS but not receiving
171 a CS at test ("No-CS"), and animals that were conditioned but not tested ("No-Test"). Conditioning
172 (Figure 5B) was similar to previous experiments (main effect of trial: $F_{6,258} = 77.346$, $p < 0.0001$;
173 no other main effects or interactions: F's < 1.30, p's > 0.30). As shown in Figure 5B, the groups
174 differed in their levels of conditioned freezing during the retrieval test. A repeated measures
175 ANOVA revealed a main effect of trial ($F_{6,216} = 15.54$, $p < 0.0001$), conditioning procedure ($F_{2,36}$
176 $= 11.42$, $p < 0.0001$), and a procedure × trial interaction ($F_{6,216} = 3.65$, $p < 0.0001$) (includes
177 baseline). Post-hoc analyses revealed that FW ($p < 0.0001$) and BW ($p < 0.005$) rats exhibited
178 significantly higher levels of freezing behavior than No-CS rats. Similarly, an ANOVA of average
179 freezing across the test trials (without baseline) revealed a main effect of group ($F_{2,36} = 13.76$, $p <$
180 0.0001). Post-hoc comparisons revealed significant differences between FW vs. BW ($p < 0.05$)
181 and FW vs. No-CS rats ($p < 0.0001$), as well as BW vs. No-CS animals ($p < 0.005$).

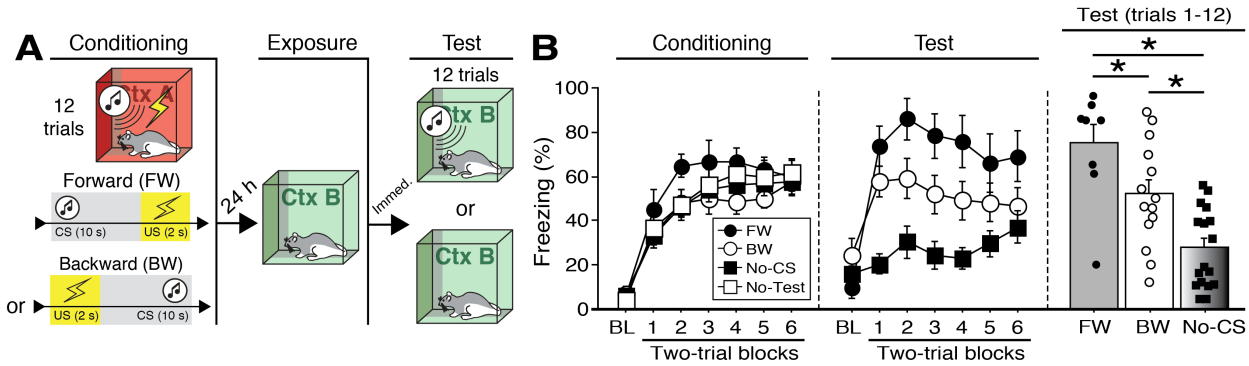

Figure 5. *CS-evoked freezing in rats utilized for Fos analyses.* **(A)** Behavioral schematic. **(B)** Freezing during conditioning and retrieval testing. For conditioning, the left panel depicts mean percentage freezing during the 5-min baseline (BL) and across each conditioning block (each block is comprised of two trials; conditioning trials consist of freezing during the 10-sec CS followed by the 58-sec interval). For retrieval testing, the center panel shows mean percentage freezing at the 5-min baseline (BL) and across each test block (each block is comprised of two trials; trials consist of freezing during the 10-sec CS followed by the 60-sec interval). The right panel shows mean percentage freezing after BL. Animals were sacrificed for Fos analyses 90 min after trial 1. All data are represented as means ± s.e.m [FW (n = 8); BW (n = 14); No-CS (n = 17); No-Test (n = 8)]; * = $p < 0.05$.

Ninety minutes after the retrieval test, the animals were sacrificed for Fos immunohistochemistry. Fos-positive nuclei were counted in three BNST subregions (Figure 6A): "ovBNST" (Fos counts confined to the oval nucleus of the BNST), "dBNST" (counts in an area containing the dorsal region of the anteromedial BNST), and "vBNST" [Fos counts in a region containing the BNST's anterolateral, fusiform, and anteromedial (ventral) nuclei; refer to (Swanson, 2003)]. As shown in Figure 6B, the average number of Fos-positive nuclei for each of these regions differed in rats undergoing FW or BW conditioning in the ovBNST and vBNST, but not the dBNST. In the vBNST, an ANOVA revealed a main effect of group ($F_{3,43}$ = 11.41, $p <$ 0.0001). Fisher's PLSD revealed that BW rats exhibited significantly higher levels of Fos compared to FW ($p < 0.0005$), No-CS ($p < 0.001$), and No-Test ($p < 0.0001$) rats. Additionally, No-CS rats exhibited significantly greater Fos expression than No-Test rats ($p < 0.05$). In the ovBNST, an ANOVA revealed a main effect of group ($F_{3,43}$ = 3.26, $p < 0.05$). Post-hoc analyses revealed that No-Test rats exhibited significantly higher Fos levels compared to FW ($p < 0.05$) and

195 No-CS ($p < 0.01$) rats. In dBNST, there was no effect of conditioning procedure on Fos expression

196 (factorial ANOVA: $F < 2.60$, $p > 0.07$). Together, these data presentation of a BW CS increases

197 Fos expression in the vBNST, an outcome that is consistent with our inactivation studies.

198 Moreover, exposure to the temporally predictive FW CS (which elicited the highest levels of fear)

199 was associated with low levels of Fos.

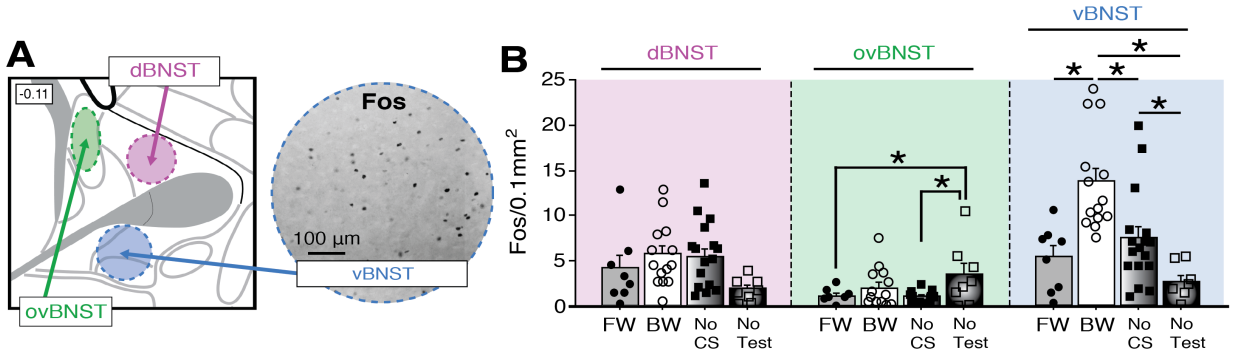

Figure 6. *Fos expression in the BNST following exposure to a temporally predictable or uncertain CS.* **(A)** Schematic depicting regions counted within the BNST (left panel). The right panel shows example of Fos expression in the ventral BNST (vBNST). **(B)** Mean Fos-positive cells per 0.1 mm^2 for each of the quantified regions. All data are represented as means ± s.e.m [FW (n = 8); BW (n = 14); No-CS (n = 17); No-Test (n = 8)]; * = $p < 0.05$.

200 ***Backward CSs selectively increase Fos expression in mPFC afferents of the BNST.*** The BNST

201 receives input from many areas involved in the regulation of fear (Fox and Shackman, 2017).

202 Therefore, we used a functional tracing procedure to quantify Fos expression in neurons targeting

203 the BNST. Specifically, rats were injected with a retrograde tracer (CTb-488) into the BNST (prior

204 to conditioning) so that we could quantify Fos expression in BNST-projecting neurons in its major

205 limbic and cortical afferents. We quantified Fos in the infralimbic (IL) and prelimbic (PL) regions

206 of the medial prefrontal cortex (mPFC), the basolateral amygdala (BLA), and the ventral

207 hippocampus (HPC; Figure 7). The behavioral data for these animals are shown in Figure 5.

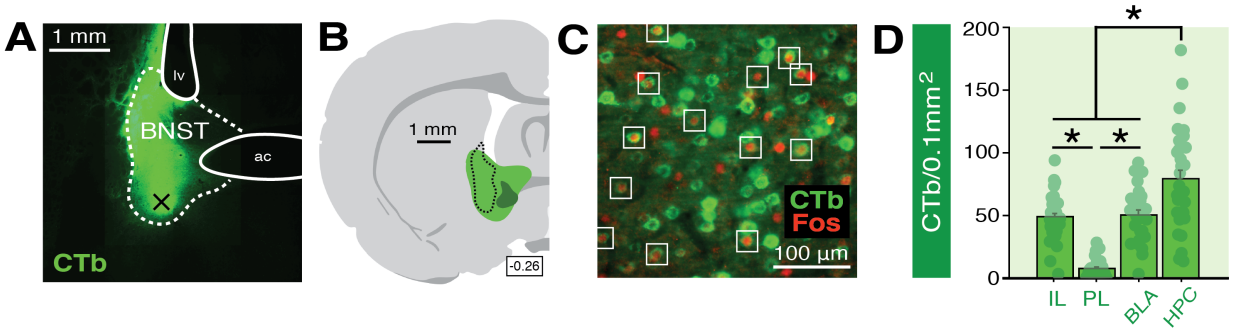

Figure 7. *Functional tracing in afferents targeting the BNST.*
(A) Coronal section (10×) showing representative fluorescence of a CTb infusion (green) into the BNST (dotted outline; "ac" = anterior commissure, "lv" = lateral ventricle). Black "X" denotes approximate lowest point of the infusion (as an example of how injection sites are documented in Figure 7—Figure Supplement 1). **(B)** Coronal schematic (-0.26 mm from bregma) showing the approximate largest (green) and smallest (dark green) areas of CTb spread in the BNST for animals included in the analyses; the black dotted outline represents the extent of spread of CTb in the BNST in the image shown in panel **A**. **(C)** Example CTb-positive (green) and Fos-positive (red; nuclei) cells in a coronal section (40 µm) of the IL; open white squares denote double-labeled cells. **(D)** Mean number of BNST-targeting CTb-positive cells (per 0.1 mm^2) for each of the quantified regions (shows FW, BW, and No-Test animals corresponding to Figure 8). All data are represented as means ± s.e.m (for each region, $n = 30$); * = $p < 0.05$.

208 A representative image of CTb infusion into the BNST is shown in Figure 7A and an
209 illustration of the largest and smallest CTb spread of injection included in the analyses is shown
210 in Figure 7B. Approximate microinjection sites for CTb for all animals are shown in Figure 7—
211 Figure Supplement 1. Representative Fos and CTb co-labeling is shown in Figure 7C. CTb counts
212 in each region did not differ by behavioral condition (F's < 0.5, p's > 0.75) and were collapsed for
213 this analysis. As shown in Figure 7D, there were reliable differences in CTb labeling among the
214 BNST afferents we quantified. An ANOVA revealed a significant main effect of region ($F_{3,116}$ =
215 42.34, $p < 0.0001$). Post-hoc comparisons indicated that the number of CTb-positive cells in the
216 HPC were significantly higher than that in all other regions ($p < 0.0001$, per comparison); IL and
217 BLA exhibited significantly greater CTb counts compared to PL ($p < 0.0001$, per comparison).
218 These data indicate extensive connectivity of the PFC, BLA, and HPC with the BNST.
219 As shown in Figure 8A, the number of Fos-positive nuclei in the IL, PL, HPC, and BLA
220 differed among the behavioral groups. Factorial ANOVA of Fos counts in IL revealed a main

221 effect of group ($F_{2,27}$ = 8.55, p < 0.005). Post-hoc comparisons for IL revealed significant
222 differences between BW vs. No-Test rats (p < 0.0005) and FW vs. No-Test rats (p < 0.05). In PL,
223 a main effect of group was also identified (factorial ANOVA: $F_{2,27}$ = 6.79, p < 0.005). Post-hoc
224 analyses indicated that BW rats exhibited significantly more Fos in PL as compared to No-Test
225 animals (p < 0.001). For BLA, a main effect of group was detected (factorial ANOVA: $F_{2,27}$ =
226 8.10, p < 0.005). Post-hoc analyses revealed that FW and BW rats (which did not significantly
227 differ) exhibited significantly more Fos in BLA as compared to No Test rats (p < 0.01, FW vs. No-
228 Test; p < 0.001, BW vs. No-Test). In HPC, an ANOVA revealed a significant main effect of group
229 ($F_{2,27}$ = 4.28, p < 0.05). Post-hoc comparisons indicated that FW and BW rats (again, which did
230 not significantly differ) had significantly more Fos expression in HPC as compared to No-Test
231 animals (p < 0.05 for FW vs. No-Test and BW vs. No-Test). These data indicate that conditioned
232 freezing to forward or backward CSs increased the number of Fos-positive neurons in the PFC,
233 BLA, and HPC.

234 To quantify the fraction of BNST-projecting neurons within the PFC, BLA, and HPC that
235 were activated by a FW or BW CS, we calculated a ratio of Fos-positive to CTb-positive nuclei in
236 each afferent region ("Fos-CTb%"; Figure 8B). Interestingly, within the IL, animals in the BW
237 group exhibited the highest fraction of double-labeled cells. An ANOVA revealed a significant
238 main effect of group ($F_{2,27}$ = 14.22, p < 0.0001). Post-hoc comparisons revealed significant
239 differences between BW and FW rats (p < 0.005) as well as BW and No-Test animals (p < 0.0001).
240 In contrast, there were no differences between FW and BW rats in any of the other regions
241 quantified. In PL, there was not a significant main effect of group (F < 1.90, p > 0.17) and no
242 group effects were observed in the BLA (F < 2.0, p > 0.15). In the HPC, rats in the FW and BW
243 groups exhibited greater numbers of double-labeled cells than those in the No-Test group ($F_{2,27}$ =

244 7.82, $p < 0.01$). Accordingly, these data indicate that conditioned freezing (in both FW and BW

245 rats) is associated with increased activity in BNST-targeting cells of HPC, and that BW CSs

246 selectively increase Fos in BNST-projecting neurons in IL. Hence, IL projections to the BNST

247 may mediate the effects of BW CSs on BNST Fos expression and freezing.

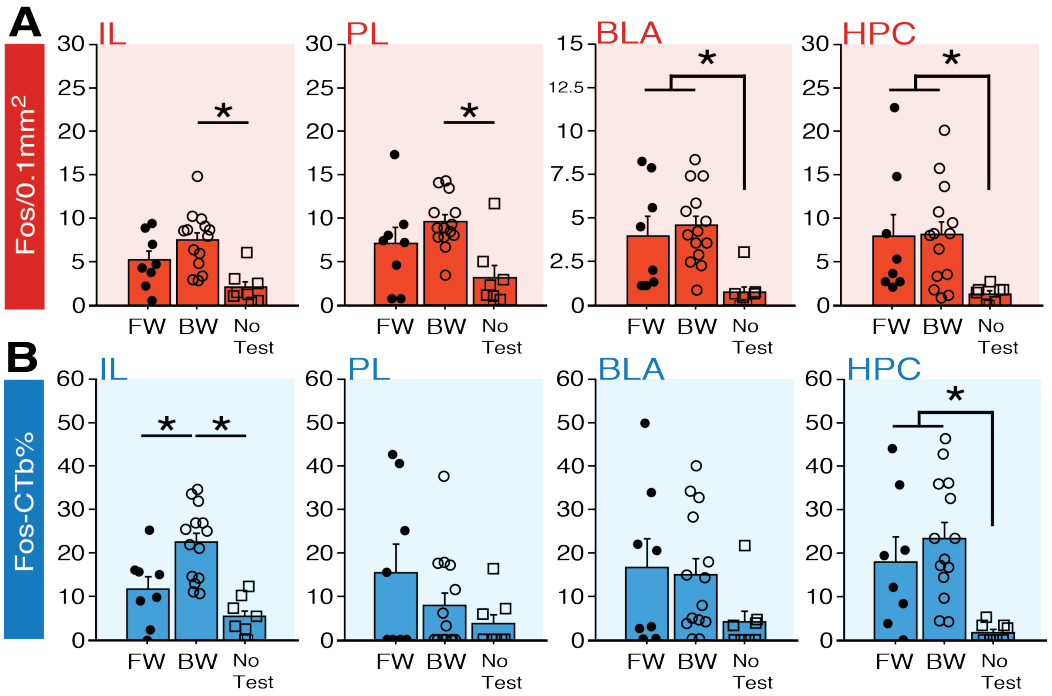

Figure 8. *Fos expression in BNST-targeting cells of prefrontal cortex, amygdala, and hippocampus following exposure to a temporally predictable or uncertain CS.* **(A)** Mean number of Fos-positive cells (per 0.1 mm^2) for each of the quantified regions. **(B)** Mean percentage of Fos-positive and CTb-positive cells divided by the total number of CTb-positive cells for each region. All data are represented as means ± s.e.m [FW (n = 8); BW (n = 14); No-Test (n = 8)]; * = $p < 0.05$.

248 **DISCUSSION**

249

250 In the present study, we demonstrate that the BNST is critical for processing ambiguous threats,

251 specifically discrete auditory cues that poorly predict when aversive footshocks will occur.

252 Reversible inactivation of the BNST inactivation disrupted conditioned freezing to a backward

253 CS, but did not affect freezing to a CS that reliably predicted the timing of shock onset even when

254 that CS signaled an unpredictable intensity of the US. Interestingly, freezing to the backward CS
255 was less sustained than that to the forward CS, suggesting that neither long-duration stimuli nor
256 sustained freezing responses are required to recruit the BNST. Finally, although both forward and
257 backward CSs increased Fos expression in the hippocampus, BNST, amygdala, and mPFC, only
258 backward CSs selectively increased Fos expression in both the ventral BNST and BNST-
259 projecting neurons in the infralimbic cortex. Collectively, these data reveal that the BNST and its
260 mPFC afferents mediate defensive responses to ambiguous threats.

261 Unpredictability comes in many forms (Bennett et al., 2018; Davies and Craske, 2015;
262 McNally et al., 2011; Schroijen et al., 2016), but uncertainty about the onset of aversive events has
263 been linked to anxiety (Bennett et al., 2018). For example, work in both humans (Shankman et al.,
264 2011) and animals (Amadi et al., 2017) suggests that unpredictable timing of aversive stimuli is a
265 key contributor to anxious symptoms. Ambiguous threats have been found to increase regional
266 cerebral blood flow in the human BNST (Alvarez et al., 2015; Klumpers et al., 2017) and BNST
267 lesions or inactivation in animals reduce defensive responses to a broad spectrum of stimuli
268 (contexts and cues) that poorly predict when aversive events will occur (Davis and Walker, 2014;
269 Goode et al., 2015; Hammack et al., 2015; Luyten et al., 2011; Sullivan et al., 2004; Waddell et
270 al., 2006; Zimmerman and Maren, 2011). It has been suggested that ambiguous signals for threat
271 induce states of anxiety, because they predict that, but not when, an aversive event might occur.
272 In the present study, backward CSs, which are ambiguous signals for the onset of aversive
273 footshocks, drove conditioned freezing that was presumably associated with a state of anticipatory
274 anxiety. Consistent with this possibility, we observed significant differences in shock reactivity
275 during forward and backward conditioning. During backward conditioning, rats exhibited more
276 robust shock-elicited activity bursts than during forward conditioning, which suggests that

277 uncertainty about the timing of aversive USs increases their aversiveness. A critical finding in the
278 present study is that the BNST mediates conditioned freezing to short-duration discrete CSs, but
279 only when those CSs are poor predictors of shock onset. This contrasts with prior work suggesting
280 that the BNST only mediates freezing behavior to long-duration cues or contexts (Hammack et al.,
281 2015; Waddell et al., 2006). However, recent data in other paradigms suggest a role for the BNST
282 in threat responses to relatively brief stimuli (Brinkmann et al., 2018; Kiyokawa et al., 2015; Luyck
283 et al., 2017). Together, these data suggest that stimulus duration is not necessarily a determinant
284 of BNST involvement. Similarly, it does not appear that response duration is a determinant of
285 BNST in threat reactions. In the present work, conditioned freezing to the backward CS was
286 generally shorter-lived than that to the forward CS, but was more sensitive to BNST inactivation
287 than freezing to the forward CS. One might conclude from this observation that the BNST mediates
288 weak (but not strong) freezing responses. However, we and others have shown that BNST lesions
289 or inactivation reduce the expression of freezing when those levels are high (Goode et al., 2015;
290 Hammack et al., 2015). Hence, the BNST mediates fear to cues that signal uncertain threat,
291 independent of the duration of the antecedent stimuli or behavioral responses associated with the
292 threat (Goode and Maren, 2017).

293 Interestingly, it has been suggested that fear to a backward CS relies on associations
294 between the CS and the conditioning context (Chang et al., 2003), which more strongly predicts
295 the US. Thus, it is possible that the BNST mediates fear expression to a backward CS by retrieving
296 a memory of the context-US association. Consistent with this, increases in immediate early gene
297 expression and metabolic activity have been observed in the BNST in response to conditioned
298 contexts (Campeau et al., 1997; Lemos et al., 2010; Luyten et al., 2012) and BNST lesions or
299 inactivation impair defensive responses to a variety of contextual stimuli (Davis and Walker, 2014;

300 Goode et al., 2015; Hammack et al., 2015; Luyten et al., 2011; Sullivan et al., 2004; Waddell et
301 al., 2006; Zimmerman and Maren, 2011). If the backward CS functions similarly to a conditioned
302 context, then one might expect Fos activity to be elevated in the BNST of animals exposed to the
303 backward CS. Indeed, we observed significantly more Fos expression in the BNST in response to
304 the backward compared to forward CS. The backward CS-elicited Fos expression was specific to
305 vBNST, insofar as backward and forward rats did not differ in overall levels of Fos in dBNST or
306 ovBNST. Others have shown elevated Fos expression in regions in or near vBNST after stress
307 (Sterrenburg et al., 2012; Verma et al., 2018), which is consistent with the greater aversion
308 embodied by a temporally unpredictable CS. Of course, another possibility is that the backward
309 conditioning procedure yielded forward trace conditioning (Burman et al., 2014; Marchand et al.,
310 2004; Raybuck and Lattal, 2014; Tipps et al., 2014). Although there has been considerable work
311 on the neural mechanisms of trace conditioning (Raybuck and Lattal, 2014), a role for the BNST
312 in this form of learning has not yet been established. Because trace conditioning also degrades the
313 temporal predictability of the CS, it might be expected to require the BNST. In either event, the
314 BNST appears to be recruited by stimuli, whether cues or contexts, that are poor predictors of
315 when aversive USs will occur.

316 The amygdala, PFC, and hippocampus have strong connections with the BNST (Canteras
317 and Swanson, 1992; deCampo and Fudge, 2013; Dong et al., 2001; Glangetas et al., 2017;
318 McDonald et al., 1999; Reichard et al., 2017; Reynolds and Zahm, 2005; Torrisi et al., 2015;
319 Vertes, 2004; Weller and Smith, 1982). In line with previous work, the expression of freezing
320 (whether elicited by a forward or backward CS) increased the number of Fos-positive neurons in
321 these regions (Herry et al., 2008; Jin and Maren, 2015; Knapska and Maren, 2009; Lemos et al.,
322 2010; Wang et al., 2016). In addition, we found that forward and backward CSs increased Fos

323 expression in BNST-targeting cells of BLA and HPC. HPC and BLA projections to the BNST are
324 thought to regulate hypothalamic-pituitary-adrenal (HPA)-axis activity (Crestani et al., 2013;
325 Forray and Gysling, 2004; Zhu et al., 2001), and these afferents may be engaged in high-fear states
326 to mobilize corticosterone release. However, unlike the HPC and BLA, we observed a greater
327 number of Fos-positive cells in the IL in response to a backward relative to forward CS. This
328 suggests a unique role for BNST-projecting neurons in the IL in processing unpredictable threats.
329 IL projections to the BNST are known to be glutamatergic (Crowley et al., 2016; Glangetas et al.,
330 2017) and activity in the IL regulates anxiety (Glangetas et al., 2017). Indeed, the present data
331 suggest that the IL may be involved in generating defensive behaviors to the backward CS. This
332 would stand in contrast to considerable data indicating that the IL is involved in the inhibition of
333 freezing behavior after extinction, for example (Milad and Quirk, 2002; Quirk and Mueller, 2008).
334 An alternative view is that the IL is involved in processing contextual information conveyed by
335 the hippocampus (Corcoran and Quirk, 2007; Marek et al., 2018; Zelikowsky et al., 2013) during
336 threat processing. To the extent that that backward CSs elicit fear via CS-(context-US) associations
337 (Chang et al., 2003), it is possible that the IL is involved in retrieving CS-context associations.

338 In conclusion, we demonstrate a novel role for the BNST processing cues that signal
339 uncertain threats. BNST inactivation impaired conditioned freezing to a backward, but not
340 forward, auditory CS that differed only in their temporal relationship to a footshock US. This
341 reveals that neither stimulus modality nor duration (or response duration) are the critical
342 parameters driving BNST involvement in defensive behavior. Moreover, BNST inactivation did
343 not affect freezing to a forward CS that was paired with a US that varied in intensity, suggesting
344 that uncertainty *per se* does not drive BNST-dependent behavior. Rather, it would appear that
345 stimuli that signal temporally uncertain threats (i.e., ambiguous threats) elicit BNST-dependent

346 freezing behavior. We further show that backward CSs increase the number of Fos-positive
347 neurons in the vBNST and in BNST-projecting neurons in the infralimbic cortex. This suggests a
348 novel role for mPFC projections to the BNST in processing ambiguous threats, possibly of the
349 aversive contexts to which backward CSs are associated. In total, these experiments provide new
350 insight into the antecedents for BNST-dependent defensive behavior and reveal novel behavioral
351 procedures to explore these processes.
352
353 **MATERIALS AND METHODS**
354
355 **Subjects.** All experiments used adult (200-240 g upon arrival; n = 215, before exclusions) male
356 Long-Evans rats (Envigo; Indianapolis, IN). Rats were housed in a climate-controlled vivarium
357 and kept on a fixed light/dark cycle (lights on starting at 7:00 AM and off at 9:00 PM; experiments
358 took place during the light phase of the cycle). Rats were individually housed in clear plastic cages
359 (with bedding consisting of wood shavings; changed weekly) on a rotating cage rack. Group
360 assignments for behavioral testing was randomized for cage position on the racks. Animals had
361 access to standard rodent chow and water *ad libitum*. Animals were handled by the experimenter(s)
362 (~30 sec/day) for five consecutive days prior to the start of any surgeries or behavior. All
363 procedures were in accordance with the US National Institutes of Health (NIH) Guide for the Care
364 and Use of Laboratory Animals and were approved by the Texas A&M University Institutional
365 Animal Care and Use Committee.
366
367 **Apparatuses.** All behavioral testing occurred within distinct rooms in the laboratory. Each
368 behavioral room housed eight identical rodent conditioning chambers (30 cm × 24 cm × 21 cm;

369 MED Associates, Inc.). Each chamber was housed in a larger, external sound-attenuating cabinet.
370 Rear walls, ceilings, and the front doors of the testing chambers were made of Plexiglas, while
371 their sidewalls were made of aluminum. Grid floors of the chambers were comprised of nineteen
372 stainless steel bars (4 mm in diameter), and spaced 1.5 cm apart (center to center). The grid floors
373 were attached to an electric shock source and a solid-state grid scrambler for delivery of the US
374 (MED Associates, Inc.). A speaker attached to each chamber was used to deliver the auditory CS.
375 As needed for each context, the chambers were equipped with 15 W house lights, and small fans
376 were embedded in the cabinets (providing background noise of ~70 dB). An aluminum pan was
377 inserted beneath the grid floor to collect animal waste. A small camera was attached to the top of
378 the cabinet for video monitoring of behavior.

379 Measurements of freezing were performed using an automated system (Maren, 1998).
380 Specifically, each behavioral testing chamber rested on a load-cell platform that was sensitive to
381 cage displacement due to the animal's movements. During behavioral testing, load-cell activity
382 values (ranging from -10 to +10 V) were collected and digitized at 5 Hz using Threshold Activity
383 Software (MED Associates, Inc.). Offline conversions of the load-cell activity values were
384 performed to generate absolute values ranging from 0 to 100; lower values indicate minimal cage
385 displacement, which coincided with freezing behaviors in the chambers. Accordingly, freezing
386 bouts were defined as absolute values of ≤10 for 1 s or more. The percentage of freezing behavior
387 during the pre-CS baseline, the CS, and the inter-trial intervals was computed for each behavioral
388 session. Shock reactivity was analyzed by directly reporting the absolute values generated by the
389 Threshold Activity Software (i.e., larger values indicated more movement in the cage).

390 Unique contexts (A and B) were used for conditioning retrieval testing. Chamber
391 assignments were unique to each context and group assignments were counterbalanced across test

392 chambers when possible. For each experiment, context A was assigned to one of the behavioral
393 rooms, and B the other. For context A, the test chamber was wiped down with an acetic acid
394 solution (3%) and a small amount was poured in the pans beneath the grid floors. The cage lights
395 were turned on, while the chamber fans were turned off. The cabinet doors were closed. The
396 behavioral room was illuminated with dim red light. Animals were transported to and from the
397 chambers using white plastic transport boxes. For context B, an ammonium hydroxide solution
398 (1%) was used to wipe down and scent the chambers, black Plexiglas panels were placed over the
399 grid floors, the cage lights were turned off, the chamber fans were turned on, and the cabinet doors
400 remained open. The behavioral room was illuminated with white light (red room lights were turned
401 off). Rats were transported to and from the context using black plastic transport boxes that included
402 a layer of clean bedding.
403
404 **Surgeries.** For animals receiving intracranial microinfusions into the BNST, rats were transported
405 to the surgical suite and deeply anesthetized using isoflurane (5% for induction, 1-2% for
406 maintenance) (Acca et al., 2017; Goode et al., 2015; Nagaya et al., 2015; Zimmerman and Maren,
407 2011). Rats were then secured in a stereotaxic frame (Kopf Instruments). Hair on top of the
408 rodent's head was shaved, povidone-iodine was applied, and a small incision was made in the scalp
409 to expose the skull. Bregma and lambda were aligned on a horizontal plane, and small holes were
410 drilled in the skull for the placement of anchoring screws and bilateral stainless-steel guide
411 cannulas (26 gauge, 8 mm from the bottom of their plastic pedestals; Small Parts). The cannulas
412 were inserted into the BNST at the following coordinates: -0.15 mm posterior to bregma, ±2.65
413 mm lateral to the midline, and -5.85 mm dorsal to dura (guide cannulas were angled at 10° with
414 their needles directed at the midline). Dental cement was used to secure the cannulas to the screws

415 and stainless steel obturators (33 gauge, 9 mm; Small Parts) were inserted into the guide cannulas.
416 Animals were given at least one week to recover prior to the onset of behavioral training.
417 For rats injected with cholera toxin subunit B (CTb) conjugated with Alexa Fluor-488
418 (CTb-488; ThermoFisher Scientific) in the BNST, the surgical procedures were identical to those
419 described above. A single small hole was drilled into the skull to allow for the insertion of glass
420 micropipettes. Injection tips were backfilled with mineral oil and secured in the injector; CTb-488
421 was then drawn up into the injector immediately before use. Rats received unilateral CTb-488
422 infusions into either the left or right hemisphere (group assignments were randomized for sites of
423 CTb-488 infusion): -0.15 mm posterior to bregma, ±2.65 mm lateral to the midline, and -6.50 mm
424 dorsal to dura (the pipette was angled at 10° with the tip directed at the midline). CTb-488 (5.0
425 mg/µl; total volume of 0.25 µl) was microinfused into the brain using a Nanoject II auto-nanoliter
426 injector (Drummond Scientific Co.) secured to the arms of the stereotaxic frame. For the infusion
427 process, 50 nl (25 nl/s) of CTb-488 was infused once per min for 5 min to achieve 0.25 µl of total
428 infusion (the injection needle was left in the brain for 5 additional minutes to allow for diffusion
429 of CTb-488). Following the infusion procedures, the incision closed with sutures and the animals
430 were returned to their homecages where they recovered for ~10 days.
431
432 **Intracranial infusions.** Prior to behavioral testing, the animals were acclimated to the process of
433 intracranial infusions. On two occasions, the animals were transported from the vivarium to the
434 infusion room in 5-gallon buckets containing a layer of bedding; the experimenter(s) removed the
435 obturators and replaced them with clean ones. On the day of infusions, animals (in squads of four
436 to eight rats; representing all drug/behavioral groups as possible) were transported to the
437 laboratory, obturators were removed, and injectors were inserted into the guides. Stainless steel

438 injectors (33 gauge, Small Parts; 9-mm extending 1 mm beyond the end of the guide cannula) were
439 connected to polyethylene tubing (PE-20; Braintree Scientific); the other end of the tubing was
440 connected to gastight 10 µl syringes (Hamilton, Co.). The syringes were mounted to an infusion
441 pump (KD Scientific, Inc.). For the experiments shown in Figure 1 and Figure 2, the α-amino-3-
442 hydroxy-5-methyl-4-isoxazolepropionic acid (AMPA) receptor antagonist 2,3-dihydroxy-6-nitro-
443 7-sulfamoyl-benzo[f]quinoxaline-2,3-dione (NBQX) was used to reversibly inactivate the BNST
444 (Adami et al., 2017; Davis and Walker, 2014; Goode et al., 2015; Zimmerman and Maren, 2011).
445 NBQX disodium salt hydrate (Sigma Life Sciences) was dissolved in saline to a concentration of
446 10.0 µg/µl ("NBQX" for Figure 1 and Figure 2); physiological saline served as the vehicle ("VEH"
447 for all experiments). For the experiments shown in Figure 4, the γ-aminobutyric acid $(GABA)_A$
448 receptor agonist muscimol was used to reversibly inactivate the BNST (Bangasser et al., 2005;
449 Breitfeld et al., 2015; Buffalari and See, 2011; Fendt et al., 2003; Goode et al., 2015; Markham et
450 al., 2009; Pina et al., 2015; Sajdyk et al., 2008; Xu et al., 2012). Muscimol (Sigma-Aldrich) was
451 dissolved in physiological saline to a concentration of 0.1 µg/µl ("MUS" for Figure 4);
452 physiological saline served as the vehicle ("VEH"). For the representative image showing drug
453 spread in the BNST (Figure 1—Figure Supplement 1), muscimol TMR-X conjugate (Thermo
454 Fisher Scientific) was dissolved in physiological saline to a concentration of 0.1 µg/µl and used
455 for infusions. For all of the aforementioned experiments, drug or vehicle was drawn into the
456 injectors (immediately prior to the infusions) and a total volume of 0.275 µl/hemisphere of drug
457 or vehicle was infused at a rate of 0.275 µl/min; injectors were left in the cannulas for 1 min
458 following the infusions to allow for diffusion. Once the injectors were removed, clean obturators
459 were inserted into the guides.
460

461 **Behavioral procedures and exclusions.** Overviews of each behavioral experiment are provided
462 in the figures. The conditioned stimulus (CS) for all experiments was an auditory tone (80 dB, 2
463 kHz, 10 sec), which was paired with a footshock the unconditioned stimulus (US, 1.0 mA, 2 sec).
464 For the variable shock intensity experiment (Figure 4), US intensity varied.

465 *FW/BW BNST inactivation (twelve training trials).* In a 3 × 2 design, animals (n = 64, prior
466 to exclusions) were randomly assigned to receive a CS at test [either a forward ("FW")- or
467 backward ("BW")-trained CS] or no CS at test [animals were trained to a BW CS; "No-CS"], and
468 NBQX ("NBQX") or vehicle infusions ("VEH"). Of these rats, seven were excluded due to off-
469 target cannulas, three additional rats were excluded due to illness, and four more were excluded
470 due to a technical error during infusions that resulted in no drug or vehicle to be infused (fourteen
471 total exclusions). This resulted in the following (final) group numbers (shown in data/figures):
472 FW-NBQX (n = 4); FW-VEH (n = 5); BW-NBQX (n = 12); BW-VEH (n = 13); No-CS-NBQX
473 (n = 8), No-CS-VEH (n = 8). For conditioning, animals (in squads of eight rats) were transported
474 from the vivarium to context A; FW and BW procedures were run in alternating squads of animals.
475 Drug and vehicle assignments were counterbalanced for position in the chambers. For FW
476 conditioning, were placed in the context for 5 min before the delivery of twelve CS-US trials (CS
477 offset immediately preceded US onset; 70-sec intertrial interval). After the final conditioning trial,
478 the animals remained in the chamber for 1 min before being returned to their homecages (the entire
479 conditioning session consisted of 19 min total; for both FW and BW conditioning). For BW
480 conditioning, all aspects of conditioning were identical to the FW training except the order of the
481 CS and US was reversed. That is, after a 5-min baseline period, the animals received 12 US-CS
482 trials (the onset of the CS occurred immediately after the offset of the US; 70-sec intertrial
483 intervals). After conditioning, rats were returned to their homecages.

484 Twenty-four hours after conditioning, animals (in squads of four) were infused with DRUG
485 or VEH into the BNST immediately before being placed in context B. After 5 min of acclimation
486 to the context, FW and BW animals (intermixed in each squad) received twelve presentations of
487 the CS in the absence of the US (70-sec intertrial interval). The rats remained in the chambers for
488 1 min following the final CS (19 min session, in total). For rats not receiving the CS at test, the
489 animals remained in the test context for 19 min without presentation of the CS or US. We alternated
490 running squads that received the CS and those that did not after the infusions. Following the test,
491 animals were returned to their homecages.

492 *FW/BW BNST inactivation (five training trials).* In a 2 × 2 design, animals (n = 28, prior
493 to exclusions) were randomly assigned to receive forward ("FW") or backward ("BW")
494 conditioning, and NBQX ("NBQX") or vehicle infusions ("VEH"). Of these rats, three were
495 excluded due to off-target cannulas. This resulted in the following (final) group numbers (shown
496 in data/figures): FW-NBQX (n = 6); FW-VEH (n = 6); BW-NBQX (n = 6); BW-VEH (n = 7). At
497 the start of behavior, rats (in squads of seven) were transported from the vivarium and placed in
498 context A. We alternated squads that received forward or backward conditioning. For forward
499 conditioning, rats were given 3 min of acclimation to the context prior to the onset of five CS-US
500 trials. Rats remained in the chamber for 1 min following the final trial (530 sec total conditioning
501 session). For backward conditioning, rats were placed in context a for a 3-min baseline (530 sec
502 session total), after which they received five US-CS trials. Rats were returned to their homecages
503 after conditioning. Twenty-four hours after conditioning, the animals were placed in context B in
504 the absence of the CS or US for 530 sec to acclimate them to the test context. After this acclimation
505 session, rats were again returned to their homecages.

506 Forty-eight hours after conditioning, the animals received NBQX or VEH infusions
507 (identical to above) immediately prior to retrieval testing. FW and BW animals were intermixed
508 in each squad. Immediately after the infusions, animals were placed in context B for a retrieval
509 test to assess freezing to the CS. The test (530 sec in total) consisted of a 3-min baseline period
510 followed by five CS-alone presentations (70-s intertrial interval). Rats were returned to their
511 homecages following the test session.

512 *FIXED/VARIABLE shock w/ BNST inactivation.* In a 2 × 2 design, rats (*n* = 31, prior to
513 exclusions) were randomly assigned to receive forward conditioning with consistent ("FIXED")
514 or variable magnitudes of the US ("VARIABLE"); muscimol ("MUS") or vehicle infusions
515 ("VEH") were made prior to retrieval testing. For FIXED animals, US intensity was 1 mA. For
516 VARIABLE animals, shock intensity (in mA) varied across trials in this order (mean = 1 mA):
517 0.5, 1.8, 0.4, 1.6, 1.4, 0.3, 0.5, 1.8, 0.4, 1.6, 1.4, 0.3. In this experiment, one rat was excluded due
518 to off-target cannulas. This resulted in the following (final) group numbers (shown in data/figures):
519 FIXED-MUS (*n* = 8); FIXED-VEH (*n* = 7); VARIABLE-MUS (*n* = 8); VARIABLE-VEH (*n* =
520 7). For conditioning, animals (in squads of seven to eight) were transported to context A (squads
521 alternated between FIXED and VARIABLE paradigms). The rats were given 5 min to acclimate
522 to the context before the onset of 12 CS-US pairings (70-sec intertrial intervals). Rats remained in
523 the chambers for 1 min following the final CS, with the entire conditioning session lasting 19 min.
524 Rats were returned to their homecages following conditioning.

525 Twenty-four hours later, rats (in squads of seven to eight) received intracranial infusions
526 of MUS or VEH into the BNST immediately before being placed in context B for retrieval testing.
527 Rats were given a 5-min baseline period before the onset of twelve CS-alone presentations (70-

528 sec intertrial intervals). Rats remained in the chambers for 1 min following the final CS, with the
529 entire test session lasting 19 min. Rats were returned to their homecages following the test.

530 *FW/BW Fos-CTb.* Animals (n = 60, before exclusions) were randomly assigned to receive
531 a forward ("FW")- or backward ("BW")-trained CS at testing, or no CS retrieval at test ("No-CS").
532 Note that the No-CS group consists of animals that were trained to either a FW or BW CS.
533 Additionally, a group of BW-trained animals remained in their homecages ("No-Test") during the
534 final test and were sacrificed alongside the other groups. Twelve rats were excluded for either
535 excessive or off-target infusion of CTb-488 outside the borders of the BNST or an absence of CTb-
536 488 labeling in the ventral BNST. One additional rat was excluded due to a technical issue that
537 resulted in the loss of tissue at the level of the prefrontal cortex. This resulted in the following
538 (final) group numbers (shown in data/figures): FW (n = 8); BW (n = 14); No-CS [n = 17 (BW-
539 trained: n = 9; FW-trained: n = 8)]; No-Test (n = 8). For behavioral training, rats (in squads of six
540 to eight; with all groups intermixed) were transported to the laboratory and placed in context B to
541 acclimate for 5 min (no CS or US) and then returned to their homecages. Later that day, the animals
542 were transported to context A where they received twelve trials of either FW or BW fear
543 conditioning, which was identical to the other aforementioned procedures. We alternated FW and
544 BW conditioning squads. After conditioning, the rats were returned to their homecages. Twenty-
545 four hours after conditioning, all rats were exposed to context B for 20 min in the absence of the
546 CS or US to acclimate them to the test context.

547 Forty-eight hours later, FW, BW, and No-CS rats were transported to context B to receive
548 a retrieval test to the CS or were merely placed in the context (No-CS condition). Squads alternated
549 between CS and No-CS test. For rats undergoing CS retrieval, FW and BW animals (intermixed
550 in each squad) received CS trials as described previously. Rats were perfused 90 min following

551 the first CS of the test, in groups of three to four. For No-CS rats (with FW- and BW-trained
552 animals intermixed), animals were exposed to context B in the absence of the CS or US. No-CS
553 rats were perfused 95 min after being placed in the test context, in groups of three to four. No-Test
554 rats were perfused alongside groups of FW, BW, and No-CS rats. Rats were returned to their
555 homecages after testing and prior to the perfusions.

556 *FW/BW intra-shock reactivity.* Rats (n = 32, no exclusions) were randomly assigned to
557 receive forward ("FW") or backward ("BW") conditioning. No rats were excluded from this
558 experiment (no infusions occurred; n = 16, per group); only data from the conditioning session are
559 shown. Animals (in squads of eight) were transported to context A for either FW or BW
560 conditioning. Parameters for FW and BW conditioning were identical to the procedures for the
561 previous 12-trial experiments. We alternated FW and BW squads. Rats were returned to their
562 homecages following training.

563

564 **Histological procedures.** At the conclusion of behavioral testing, cannula-implanted animals were
565 overdosed with sodium pentobarbital (Fatal Plus; 100 mg/ml, 0.5 ml, i.p.). Transcardial perfusions
566 were then performed using chilled physiological saline followed by 10% formalin. Brains were
567 extracted and stored in 10% formalin for 24 hr at 4° C; brains were transferred to a 30% sucrose-
568 formalin solution for three or more days (at 4° C) before sectioning. Brains were flash frozen with
569 crushed dry ice and coronal sections (40 μm) containing the BNST were collected using a cryostat
570 (Leica Microsystems) at -20° C. The tissue was wet-mounted to gelatin-subbed microscope slides
571 and stained with 0.25% thionin prior to adding glass coverslips secured with mounting medium
572 (Permount, Sigma). To further examine the spread of drug, a subset of animals was infused
573 (identical to the aforementioned infusion parameters) with fluorescent muscimol (1.0 μg/μl;

574 EverFluor TMR-X conjugate, Setareh Biotech) before being sacrificed (these animals were not
575 perfused) and having brains dissected (40 μm; brains were stored in 30% sucrose solution at 4° C
576 until sectioning). These tissues were wet-mounted to slides and aqueous mounting medium
577 (Fluoromount; Sigma-Aldrich) was used to secure glass coverslips.

578 For CTb-injected animals, post-behavior perfusions mirrored the aforementioned
579 procedures. For sectioning, coronal sections (which included regions of the prefrontal cortex,
580 BNST, basolateral amygdala, and ventral hippocampus) were collected into well plates containing
581 phosphate-buffered saline (1× PBS) and stored in the dark at 4° C until immunohistochemistry
582 could be performed. For localization of the CTb-injection site, separate sections at the level of the
583 BNST were wet-mounted and coverslipped using Fluoromount mounting medium.

584

585 **Immunohistochemistry.** Immunohistochemistry for Fos was performed on free-floating brain
586 tissue similar to prior reports (Jin and Maren, 2015; Marek et al., 2018; Orsini et al., 2011; Wang
587 et al., 2016). For sections containing the BNST, Fos was stained using the following procedures
588 [all steps were performed at room temperature (~20° C) on a shaker, unless stated otherwise; rinses
589 were brief (~20 sec)]. The tissue was first rinsed in 1× tris-buffered saline (TBS; 7.4 pH), and then
590 incubated in 0.3% H_2O_2 (in TBS) for 15 min, followed by rinses (×3) in TBS. Slices were
591 transferred to primary antibody [rabbit anti-c-fos, 1:10,000 in 1× TBS containing Tween 20
592 (TBST); Millipore] and incubated overnight. Sections were then rinsed (×3) in TBS before
593 incubating in secondary antibody for 1 hr (biotinylated goat anti-rabbit, 1:1,000 in TBST; Jackson
594 Immunoresearch). Sections were rinsed (×3) again in TBS. The slices were transferred to wells
595 containing avidin biotin complex (ABC, 1:1,000 in TBST; Vector Labs) for 45 min. The tissues
596 were again rinsed (×3) in TBS. Tissue was transferred to wells containing 3,3′ diaminobenzidine

597 [(DAB) 5% stock, 1:200], nickel ammonium sulfate (5% stock, 1:10), and 30% H_2O_2 (1:2,000) in
598 TBS for 10 min to generate purple/black nuclear chromophore products. After another rinse (×3)
599 in TBS, the tissue was subsequently wet-mounted to slides and secured with coverslips using
600 Permount mounting medium.

601 For sections containing the prefrontal cortex, amygdala, and hippocampus (Fos-CTb
602 experiment), Fos was stained using the following procedures [unless stated otherwise, each step
603 occurred at room temperature (~20° C) on a shaker (and away from excess light)]. First, the tissue
604 was rinsed (10 min; ×2) in 1× TBS, followed by a 10 min wash in 1× TBST. The tissue was
605 incubated in 10% normal donkey serum (NDS; in TBST) for 1 hr. The slices were then rinsed (5
606 min; ×2) in TBST. Sections were transferred to primary antibody [goat anti-c-fos, 1:2,000 in 3%
607 NDS (in TBST); Santa Cruz Biotechnology] and incubated on a rotator in the dark for 72 hr at 4°
608 C. The tissue was rinsed (10 min; ×3) in TBST before incubating in secondary antibody
609 [biotinylated donkey anti-goat, 1:200 in 3% NDS (in TBST); Santa Cruz Biotechnology] for 2 hr.
610 Slices were then rinsed (10 min; ×3) in TBST. Sections were transferred to wells containing
611 streptavidin (Alexa-Fluor 594-conjugate, 1:500 in 3% NDS (in TBST); Thermo Fisher Scientific]
612 for 1 hr. Tissue was rinsed in (10 min; ×3) in TBS before being wet-mounted to slides and secured
613 with coverslips using Fluoromount mounting medium.

614

615 **Image analyses.** All imaging and counting procedures (for all regions) were performed with the
616 experimenter(s) blind to the group assignments of the animals. For thionin-stained coronal tissue,
617 photomicrographs of cannula in the BNST were generated (10× magnification) using a Leica
618 microscope (MZFLIII) and Leica Firecam software. For animals infused with fluorescent
619 muscimol into the BNST, infusion sites were imaged (10× magnification) using a Zeiss

620 microscope and Axio Imager 2 software (Zen Pro 2012). For CTb-injected animals, BNST images
621 were generated (10× magnification) using the same Zeiss microscope and software.

622 For Fos analyses in BNST, brightfield images of BNST [in BNST regions ranging from
623 approximately -0.00 to -0.50 mm posterior to bregma of the skull, and from both left and right
624 hemispheres (randomized for site of CTb-injection)] were generated (10× magnification) using a
625 Zeiss microscope and Axio Imager 2 software (Zen Pro 2012). ImageJ software (National
626 Institutes of Health) was used to count cells. Counts were confined to the following areas of
627 interest: (1) "ovBNST" [an area of 0.217 mm × 0.558 mm (oval); targeting the oval nucleus of the
628 BNST], (2) "dBNST" [0.372 mm^2 (circle); targeting the dorsal and medial subregions of the
629 anterior BNST, including the anteromedial area of the BNST (dorsal to the anterior commissure)],
630 and (3) "vBNST" [0.434 mm^2 (circle); targeting the ventral regions (ventral to the anterior
631 commissure) of the anterior BNST, which includes the ventral portion of the anteromedial area,
632 the anterolateral area, and the fusiform nucleus of the BNST] (Swanson, 2003). For each of these
633 regions, three to six images were quantified and averaged for each animal (Fos levels were
634 standardized to 0.1 mm^2).

635 For Fos-CTb analyses in the prefrontal cortex, amygdala, and hippocampus, images (10×
636 magnification) of Fos and CTb expression were generated using a Zeiss microscope and Axio
637 Imager 2 software (Zen Pro 2012), and counts were analyzed using ImageJ. Images were only
638 generated for the hemisphere injected with CTb for these areas. Counts were confined to the
639 following areas of interest: (1) "IL" [an area of 0.805 mm × 0.217 mm (rectangle); targeting deep
640 and superficial layers of the infralimbic cortex], (2) "PL" [1.115 mm × 0.217 mm (rectangle);
641 targeting deep and superficial layers of the prelimbic cortex], (3) "BLA" [0.434 mm^2 (circle);
642 targeting the basolateral amygdala, and (4) "HPC" [0.496 mm × 0.217 mm (rectangle); targeting

643 the ventral subiculum but may include some CA1 cells of the ventral hippocampus (Swanson,
644 2003). For each of these regions, three to six images were quantified and averaged for each animal
645 (all counts were normalized to 0.1 mm^2).
646
647 **Statistics.** All data were submitted to repeated or factorial analysis of variance (ANOVA) or two-
648 tailed *t*-tests as appropriate and as described for each experiment. Fisher's protected least
649 significant difference (PLSD) test was used for *post hoc* comparisons of group means following a
650 significant omnibus *F* ratio in the ANOVA (α was set at 0.05). No statistical methods were used
651 to predetermine group sizes (group sizes were selected based on prior work and what is common
652 for the field). Data distributions were assumed to be normal, but these were not formally tested.
653 Unless stated otherwise, all data are represented as means ± s.e.m.
654
655 **ACKNOWLEDGEMENTS**
656 The authors thank Carolyn Evemy, Kaitlyn French, and Sohmee Kim for technical assistance.
657 Supported by grants from the National Institutes of Health (R01MH065961 and R01MH117852
658 to S.M. and F31MH107113 to T.D.G.), as well as a McKnight Foundation Memory and Cognitive
659 Disorders Award and a Brain & Behavior Research Foundation NARSAD Distinguished
660 Investigator Grant to S.M.
661
662 **ADDITIONAL INFORMATION**
663 **Competing interests**
664 The authors declare no competing interests.
665

Author contributions

T.D.G. and S.M. designed research; T.D.G., R.R., and G.M.A. performed the research; T.D.G., R.R., G.M.A., and S.M. analyzed data; T.D.G. and S.M. wrote the paper.

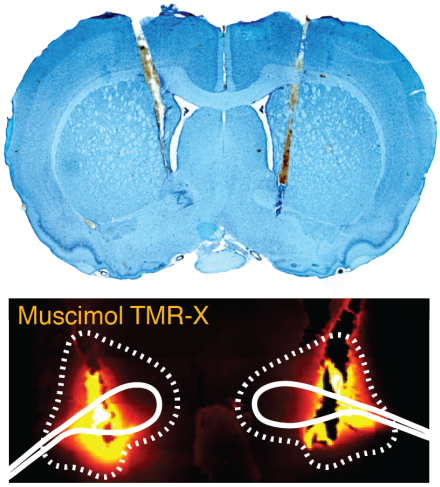

Figure 1—Figure Supplement 1
Representative bilateral cannula placements in the BNST. Photomicrograph (10×) of a thionin-stained coronal section depicting representative cannula tracts in the BNST (top panel). Fluorescent image (gold filter) of a coronal section (10×) showing spread of drug in BNST (BNST outlined in dotted line) (bottom panel).

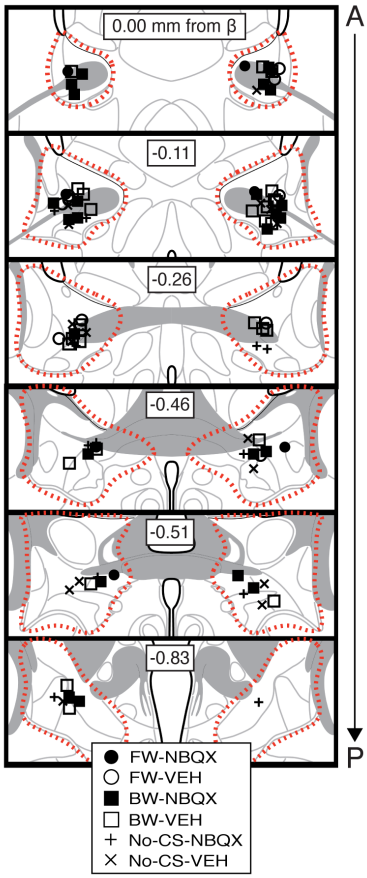

Figure 1—Figure Supplement 2
Bilateral cannula placements for BNST microinfusions. Schematic depicting cannula placements for Figure 1. Symbols (split by each group) correspond to injector tips (approximate borders of BNST are shown by red dotted outline; approximate borders of BNST are shown by red dotted outline).

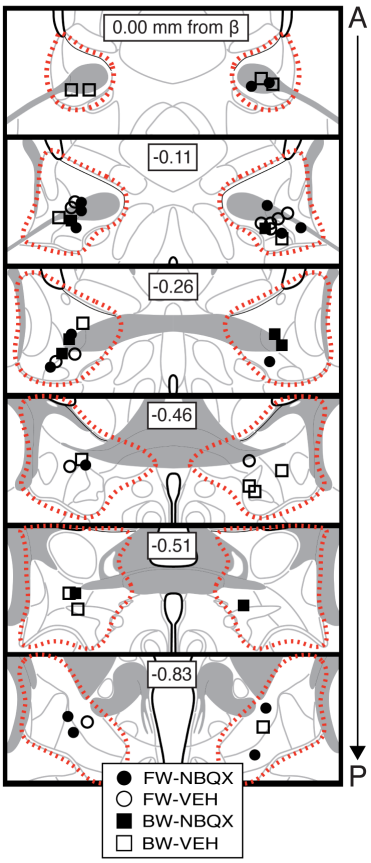

Figure 2—Figure Supplement 1
Bilateral cannula placements for BNST microinfusions. Schematic depicting cannula placements for Figure 2. Symbols (split by each group) correspond to injector tips (approximate borders of BNST are shown by red dotted outline).

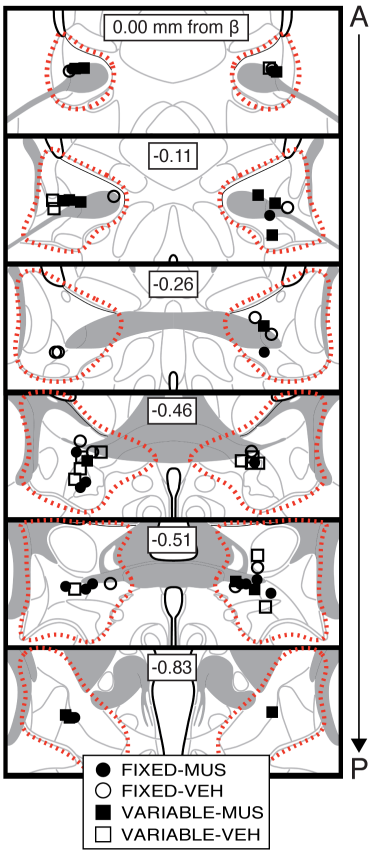

Figure 4—Figure Supplement 1
Bilateral cannula placements for BNST microinfusions. Schematic depicting cannula placements for Figure 4. Symbols (split by each group) correspond to injector tips (approximate borders of BNST are shown by red dotted outline).

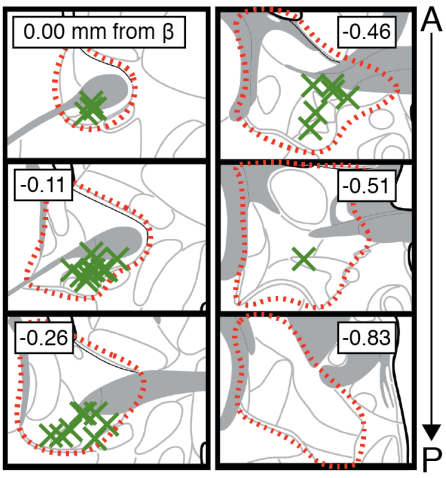

Figure 7—Figure Supplement 1
CTb injection sites in BNST. Approximation of the most ventral and centermost sites of unilateral microinjection of CTb (green X's) for all animals shown in Figure 7 (red outline approximates borders of BNST).

References

Acca, G.M., Mathew, A.S., Jin, J., Maren, S., Nagaya, N., 2017. Allopregnanolone induces state-dependent fear via the bed nucleus of the stria terminalis. Horm Behav 89, 137–144. doi:10.1016/j.yhbeh.2017.01.002

Adami, M.B., Barretto-de-Souza, L., Duarte, J.O., Almeida, J., Crestani, C.C., 2017. Both N-methyl-D-aspartate and non-N-methyl-D-aspartate glutamate receptors in the bed nucleus of the stria terminalis modulate the cardiovascular responses to acute restraint stress in rats. J Psychopharmacol (Oxford) 31, 674–681. doi:10.1177/0269881117691468

Alvarez, R.P., Kirlic, N., Misaki, M., Bodurka, J., Rhudy, J.L., Paulus, M.P., Drevets, W.C., 2015. Increased anterior insula activity in anxious individuals is linked to diminished perceived control. Translational psychiatry 5, e591. doi:10.1038/tp.2015.84

Amadi, U., Lim, S.H., Liu, E., Baratta, M.V., Goosens, K.A., 2017. Hippocampal processing of ambiguity enhances fear memory. Psychol Sci 28, 143–161. doi:10.1177/0956797616674055

Avery, S.N., Clauss, J.A., Blackford, J.U., 2016. The human BNST: functional role in anxiety and addiction. Neuropsychopharmacology 41, 126–141. doi:10.1038/npp.2015.185

Bali, A., Jaggi, A.S., 2015. Electric foot shock stress: a useful tool in neuropsychiatric studies. Rev Neurosci 26, 655–677. doi:10.1515/revneuro-2015-0015

Bangasser, D.A., Santollo, J., Shors, T.J., 2005. The bed nucleus of the stria terminalis is critically involved in enhancing associative learning after stressful experience. Behav Neurosci 119, 1459–1466. doi:10.1037/0735-7044.119.6.1459

Bennett, K.P., Dickmann, J.S., Larson, C.L., 2018. If or when? Uncertainty's role in anxious anticipation. Psychophysiology. doi:10.1111/psyp.13066

Blanco, C., Xu, Y., Schneier, F.R., Okuda, M., Liu, S.-M., Heimberg, R.G., 2011. Predictors of persistence of social anxiety disorder: a national study. J Psychiatr Res 45, 1557–1563. doi:10.1016/j.jpsychires.2011.08.004

Breitfeld, T., Bruning, J.E.A., Inagaki, H., Takeuchi, Y., Kiyokawa, Y., Fendt, M., 2015. Temporary inactivation of the anterior part of the bed nucleus of the stria terminalis blocks alarm pheromone-induced defensive behavior in rats. Front Neurosci 9, 321. doi:10.3389/fnins.2015.00321

Brinkmann, L., Buff, C., Feldker, K., Neumeister, P., Heitmann, C.Y., Hofmann, D., Bruchmann, M., Herrmann, M.J., Straube, T., 2018. Inter-individual differences in trait anxiety shape the functional connectivity between the bed nucleus of the stria terminalis and the amygdala during brief threat processing. Neuroimage 166, 110–116. doi:10.1016/j.neuroimage.2017.10.054

Brinkmann, L., Buff, C., Neumeister, P., Tupak, S.V., Becker, M.P.I., Herrmann, M.J., Straube, T., 2017. Dissociation between amygdala and bed nucleus of the stria terminalis during threat anticipation in female post-traumatic stress disorder patients. Hum Brain Mapp 38, 2190–2205. doi:10.1002/hbm.23513

Buff, C., Brinkmann, L., Bruchmann, M., Becker, M.P.I., Tupak, S., Herrmann, M.J., Straube, T., 2017. Activity alterations in the bed nucleus of the stria terminalis and amygdala during threat anticipation in generalized anxiety disorder. Soc Cogn Affect Neurosci 12, 1766–1774. doi:10.1093/scan/nsx103

Buffalari, D.M., See, R.E., 2011. Inactivation of the bed nucleus of the stria terminalis in an animal model of relapse: effects on conditioned cue-induced reinstatement and its enhancement by yohimbine. Psychopharmacology (Berl) 213, 19–27. doi:10.1007/s00213-010-2008-3

Burman, M.A., Simmons, C.A., Hughes, M., Lei, L., 2014. Developing and validating trace fear conditioning protocols in C57BL/6 mice. J Neurosci Methods 222, 111–117. doi:10.1016/j.jneumeth.2013.11.005

Campeau, S., Falls, W.A., Cullinan, W.E., Helmreich, D.L., Davis, M., Watson, S.J., 1997. Elicitation and reduction of fear: behavioural and neuroendocrine indices and brain induction of the immediate-early gene c-fos. Neuroscience 78, 1087–1104. doi:10.1016/S0306-4522(96)00632-X

Canteras, N.S., Swanson, L.W., 1992. Projections of the ventral subiculum to the amygdala, septum, and hypothalamus: a PHAL anterograde tract-tracing study in the rat. J Comp Neurol 324, 180–194. doi:10.1002/cne.903240204

Ch'ng, S., Fu, J., Brown, R.M., McDougall, S.J., Lawrence, A.J., 2018. The intersection of stress and reward: BNST modulation of aversive and appetitive states. Prog Neuropsychopharmacol Biol Psychiatry. doi:10.1016/j.pnpbp.2018.01.005

Chang, R.C., Blaisdell, A.P., Miller, R.R., 2003. Backward conditioning: mediation by the context. J Exp Psychol Anim Behav Process 29, 171–183. doi:10.1037/0097-7403.29.3.171

Colvonen, P.J., Glassman, L.H., Crocker, L.D., Buttner, M.M., Orff, H., Schiehser, D.M., Norman, S.B., Afari, N., 2017. Pretreatment biomarkers predicting PTSD psychotherapy outcomes: A systematic review. Neurosci Biobehav Rev 75, 140–156. doi:10.1016/j.neubiorev.2017.01.027

Comer, J.S., Blanco, C., Hasin, D.S., Liu, S.-M., Grant, B.F., Turner, J.B., Olfson, M., 2011. Health-related quality of life across the anxiety disorders: results from the national epidemiologic survey on alcohol and related conditions (NESARC). J Clin Psychiatry 72, 43–50. doi:10.4088/JCP.09m05094blu

Corcoran, K.A., Quirk, G.J., 2007. Activity in prelimbic cortex is necessary for the expression of learned, but not innate, fears. J Neurosci 27, 840–844. doi:10.1523/JNEUROSCI.5327-06.2007

Costello, E.J., He, J., Sampson, N.A., Kessler, R.C., Merikangas, K.R., 2014. Services for adolescents with psychiatric disorders: 12-month data from the National Comorbidity Survey-Adolescent. Psychiatr Serv 65, 359–366. doi:10.1176/appi.ps.201100518

Crestani, C.C., Alves, F.H., Gomes, F.V., Resstel, L.B., Correa, F.M., Herman, J.P., 2013. Mechanisms in the bed nucleus of the stria terminalis involved in control of autonomic and neuroendocrine functions: a review. Curr Neuropharmacol 11, 141–159. doi:10.2174/1570159X11311020002

Crowley, N.A., Bloodgood, D.W., Hardaway, J.A., Kendra, A.M., McCall, J.G., Al-Hasani, R., McCall, N.M., Yu, W., Schools, Z.L., Krashes, M.J., Lowell, B.B., Whistler, J.L., Bruchas, M.R., Kash, T.L., 2016. Dynorphin controls the gain of an amygdalar anxiety circuit. Cell Rep 14, 2774–2783. doi:10.1016/j.celrep.2016.02.069

Daldrup, T., Lesting, J., Meuth, P., Seidenbecher, T., Pape, H.-C., 2016. Neuronal correlates of sustained fear in the anterolateral part of the bed nucleus of stria terminalis. Neurobiol Learn Mem 131, 137–146. doi:10.1016/j.nlm.2016.03.020

Davies, C.D., Craske, M.G., 2015. Psychophysiological responses to unpredictable threat: effects of cue and temporal unpredictability. Emotion 15, 195–200. doi:10.1037/emo0000038

Davis, M., 2006. Neural systems involved in fear and anxiety measured with fear-potentiated startle. Am Psychol 61, 741–756. doi:10.1037/0003-066X.61.8.741

Davis, M., Walker, D.L., 2014. Role of bed nucleus of the stria terminalis and amygdala AMPA receptors in the development and expression of context conditioning and sensitization of startle by prior shock. Brain Struct Funct 219, 1969–1982. doi:10.1007/s00429-013-0616-5

Davis, M., Walker, D.L., Miles, L., Grillon, C., 2010. Phasic vs sustained fear in rats and humans: role of the extended amygdala in fear vs anxiety. Neuropsychopharmacology 35, 105–135. doi:10.1038/npp.2009.109

deCampo, D.M., Fudge, J.L., 2013. Amygdala projections to the lateral bed nucleus of the stria terminalis in the macaque: comparison with ventral striatal afferents. J Comp Neurol 521, 3191–3216. doi:10.1002/cne.23340

Deslauriers, J., Toth, M., Der-Avakian, A., Risbrough, V.B., 2017. Current status of animal models of posttraumatic stress disorder: behavioral and biological phenotypes, and future challenges in improving translation. Biol Psychiatry. doi:10.1016/j.biopsych.2017.11.019

Dong, H.W., Petrovich, G.D., Swanson, L.W., 2001. Topography of projections from amygdala to bed nuclei of the stria terminalis. Brain Res Brain Res Rev 38, 192–246. doi:10.1016/S0165-0173(01)00079-0

Fanselow, M.S., 1994. Neural organization of the defensive behavior system responsible for fear. Psychon Bull Rev 1, 429–438. doi:10.3758/BF03210947

Fanselow, M.S., Pennington, Z.T., 2017. The Danger of LeDoux and Pine's Two-System Framework for Fear. Am J Psychiatry 174, 1120–1121. doi:10.1176/appi.ajp.2017.17070818

Fanselow, M.S., Pennington, Z.T., 2018. A return to the psychiatric dark ages with a two-system framework for fear. Behav Res Ther 100, 24–29. doi:10.1016/j.brat.2017.10.012

Fendt, M., Endres, T., Apfelbach, R., 2003. Temporary inactivation of the bed nucleus of the stria terminalis but not of the amygdala blocks freezing induced by trimethylthiazoline, a component of fox feces. J Neurosci 23, 23–28.

Forray, M.I., Gysling, K., 2004. Role of noradrenergic projections to the bed nucleus of the stria terminalis in the regulation of the hypothalamic-pituitary-adrenal axis. Brain Res Brain Res Rev 47, 145–160. doi:10.1016/j.brainresrev.2004.07.011

Fox, A.S., Shackman, A.J., 2017. The central extended amygdala in fear and anxiety: Closing the gap between mechanistic and neuroimaging research. Neurosci Lett. doi:10.1016/j.neulet.2017.11.056

Gewirtz, J.C., McNish, K.A., Davis, M., 1998. Lesions of the bed nucleus of the stria terminalis block sensitization of the acoustic startle reflex produced by repeated stress, but not fear-potentiated startle. Prog Neuropsychopharmacol Biol Psychiatry 22, 625–648.

Glangetas, C., Massi, L., Fois, G.R., Jalabert, M., Girard, D., Diana, M., Yonehara, K., Roska, B., Xu, C., Lüthi, A., Caille, S., Georges, F., 2017. NMDA-receptor-dependent plasticity in the bed nucleus of the stria terminalis triggers long-term anxiolysis. Nat Commun 8, 14456. doi:10.1038/ncomms14456

Goode, T.D., Kim, J.J., Maren, S., 2015. Reversible inactivation of the bed nucleus of the stria terminalis prevents reinstatement but not renewal of extinguished fear. eNeuro 2. doi:10.1523/ENEURO.0037-15.2015

Goode, T.D., Maren, S., 2017. Role of the bed nucleus of the stria terminalis in aversive learning and memory. Learn Mem 24, 480–491. doi:10.1101/lm.044206.116

Graham, B.M., Callaghan, B.L., Richardson, R., 2014. Bridging the gap: Lessons we have learnt from the merging of psychology and psychiatry for the optimisation of treatments for emotional disorders. Behav Res Ther 62, 3–16. doi:10.1016/j.brat.2014.07.012

Gungor, N.Z., Paré, D., 2016. Functional heterogeneity in the bed nucleus of the stria terminalis. J Neurosci 36, 8038–8049. doi:10.1523/JNEUROSCI.0856-16.2016

Hammack, S.E., Guo, J.-D., Hazra, R., Dabrowska, J., Myers, K.M., Rainnie, D.G., 2009. The response of neurons in the bed nucleus of the stria terminalis to serotonin: implications for anxiety. Prog Neuropsychopharmacol Biol Psychiatry 33, 1309–1320. doi:10.1016/j.pnpbp.2009.05.013

Hammack, S.E., Todd, T.P., Kocho-Schellenberg, M., Bouton, M.E., 2015. Role of the bed nucleus of the stria terminalis in the acquisition of contextual fear at long or short context-shock intervals. Behav Neurosci 129, 673–678. doi:10.1037/bne0000088

Herry, C., Ciocchi, S., Senn, V., Demmou, L., Müller, C., Lüthi, A., 2008. Switching on and off fear by distinct neuronal circuits. Nature 454, 600–606. doi:10.1038/nature07166

Iza, M., Olfson, M., Vermes, D., Hoffer, M., Wang, S., Blanco, C., 2013. Probability and predictors of first treatment contact for anxiety disorders in the United States: analysis of data from the National Epidemiologic Survey on Alcohol and Related Conditions (NESARC). J Clin Psychiatry 74, 1093–1100. doi:10.4088/JCP.13m08361

Jin, J., Maren, S., 2015. Fear renewal preferentially activates ventral hippocampal neurons projecting to both amygdala and prefrontal cortex in rats. Sci Rep 5, 8388. doi:10.1038/srep08388

Kinley, D.J., Walker, J.R., Enns, M.W., Sareen, J., 2011. Panic attacks as a risk for later psychopathology: results from a nationally representative survey. Depress Anxiety 28, 412–419. doi:10.1002/da.20809

Kiyokawa, Y., Mikami, K., Mikamura, Y., Ishii, A., Takeuchi, Y., Mori, Y., 2015. The 3-second auditory conditioned stimulus is a more effective stressor than the 20-second auditory

conditioned stimulus in male rats. Neuroscience 299, 79–87. doi:10.1016/j.neuroscience.2015.04.055

Klumpers, F., Kroes, M.C.W., Baas, J.M.P., Fernández, G., 2017. How human amygdala and bed nucleus of the stria terminalis may drive distinct defensive responses. J Neurosci 37, 9645–9656. doi:10.1523/JNEUROSCI.3830-16.2017

Knapska, E., Maren, S., 2009. Reciprocal patterns of c-Fos expression in the medial prefrontal cortex and amygdala after extinction and renewal of conditioned fear. Learn Mem 16, 486–493. doi:10.1101/lm.1463909

Kunwar, P.S., Zelikowsky, M., Remedios, R., Cai, H., Yilmaz, M., Meister, M., Anderson, D.J., 2015. Ventromedial hypothalamic neurons control a defensive emotion state. elife 4. doi:10.7554/eLife.06633

Lange, M.D., Daldrup, T., Remmers, F., Szkudlarek, H.J., Lesting, J., Guggenhuber, S., Ruehle, S., Jüngling, K., Seidenbecher, T., Lutz, B., Pape, H.C., 2017. Cannabinoid CB1 receptors in distinct circuits of the extended amygdala determine fear responsiveness to unpredictable threat. Mol Psychiatry 22, 1422–1430. doi:10.1038/mp.2016.156

Lebow, M.A., Chen, A., 2016. Overshadowed by the amygdala: the bed nucleus of the stria terminalis emerges as key to psychiatric disorders. Mol Psychiatry 21, 450–463. doi:10.1038/mp.2016.1

LeDoux, J., Daw, N.D., 2018. Surviving threats: neural circuit and computational implications of a new taxonomy of defensive behaviour. Nat Rev Neurosci 19, 269–282. doi:10.1038/nrn.2018.22

LeDoux, J.E., Iwata, J., Cicchetti, P., Reis, D.J., 1988. Different projections of the central amygdaloid nucleus mediate autonomic and behavioral correlates of conditioned fear. J Neurosci 8, 2517–2529.

Lemos, J.I., Resstel, L.B., Guimarães, F.S., 2010. Involvement of the prelimbic prefrontal cortex on cannabidiol-induced attenuation of contextual conditioned fear in rats. Behav Brain Res 207, 105–111. doi:10.1016/j.bbr.2009.09.045

Luyck, K., Nuttin, B., Luyten, L., 2017. Electrolytic post-training lesions of the bed nucleus of the stria terminalis block startle potentiation in a cued fear conditioning procedure. Brain Struct Funct 1–10. doi:10.1007/s00429-017-1591-z

Luyten, L., Casteels, C., Vansteenwegen, D., van Kuyck, K., Koole, M., Van Laere, K., Nuttin, B., 2012. Micro-positron emission tomography imaging of rat brain metabolism during expression of contextual conditioning. J Neurosci 32, 254–263. doi:10.1523/JNEUROSCI.3701-11.2012

Luyten, L., van Kuyck, K., Vansteenwegen, D., Nuttin, B., 2011. Electrolytic lesions of the bed nucleus of the stria terminalis disrupt freezing and startle potentiation in a conditioned context. Behav Brain Res 222, 357–362. doi:10.1016/j.bbr.2011.03.066

Marchand, A.R., Luck, D., Di Scala, G., 2004. Trace fear conditioning: a role for context? Arch Ital Biol 142, 251–263.

Marek, R., Jin, J., Goode, T.D., Giustino, T.F., Wang, Q., Acca, G.M., Holehonnur, R., Ploski, J.E., Fitzgerald, P.J., Lynagh, T., Lynch, J.W., Maren, S., Sah, P., 2018. Hippocampus-

driven feed-forward inhibition of the prefrontal cortex mediates relapse of extinguished fear. Nat Neurosci 21, 384–392. doi:10.1038/s41593-018-0073-9

Maren, S., 1998. Overtraining does not mitigate contextual fear conditioning deficits produced by neurotoxic lesions of the basolateral amygdala. J Neurosci 18, 3088–3097.

Markham, C.M., Norvelle, A., Huhman, K.L., 2009. Role of the bed nucleus of the stria terminalis in the acquisition and expression of conditioned defeat in Syrian hamsters. Behav Brain Res 198, 69–73. doi:10.1016/j.bbr.2008.10.022

McDonald, A.J., Shammah-Lagnado, S.J., Shi, C., Davis, M., 1999. Cortical afferents to the extended amygdala. Ann N Y Acad Sci 877, 309–338. doi:10.1111/j.1749-6632.1999.tb09275.x

McNally, G.P., Johansen, J.P., Blair, H.T., 2011. Placing prediction into the fear circuit. Trends Neurosci 34, 283–292. doi:10.1016/j.tins.2011.03.005

Milad, M.R., Quirk, G.J., 2002. Neurons in medial prefrontal cortex signal memory for fear extinction. Nature 420, 70–74. doi:10.1038/nature01138

Nagaya, N., Acca, G.M., Maren, S., 2015. Allopregnanolone in the bed nucleus of the stria terminalis modulates contextual fear in rats. Front Behav Neurosci 9, 205. doi:10.3389/fnbeh.2015.00205

Nees, F., Heinrich, A., Flor, H., 2015. A mechanism-oriented approach to psychopathology: The role of Pavlovian conditioning. Int J Psychophysiol 98, 351–364. doi:10.1016/j.ijpsycho.2015.05.005

Orsini, C.A., Kim, J.H., Knapska, E., Maren, S., 2011. Hippocampal and prefrontal projections to the basal amygdala mediate contextual regulation of fear after extinction. J Neurosci 31, 17269–17277. doi:10.1523/JNEUROSCI.4095-11.2011

Perusini, J.N., Fanselow, M.S., 2015. Neurobehavioral perspectives on the distinction between fear and anxiety. Learn Mem 22, 417–425. doi:10.1101/lm.039180.115

Pina, M.M., Young, E.A., Ryabinin, A.E., Cunningham, C.L., 2015. The bed nucleus of the stria terminalis regulates ethanol-seeking behavior in mice. Neuropharmacology 99, 627–638. doi:10.1016/j.neuropharm.2015.08.033

Pine, D.S., LeDoux, J.E., 2017. Elevating the role of subjective experience in the clinic: response to fanselow and pennington. Am J Psychiatry 174, 1121–1122. doi:10.1176/appi.ajp.2017.17070818r

Quirk, G.J., Mueller, D., 2008. Neural mechanisms of extinction learning and retrieval. Neuropsychopharmacology 33, 56–72. doi:10.1038/sj.npp.1301555

Rabellino, D., Densmore, M., Harricharan, S., Jean, T., McKinnon, M.C., Lanius, R.A., 2018. Resting-state functional connectivity of the bed nucleus of the stria terminalis in post-traumatic stress disorder and its dissociative subtype. Hum Brain Mapp 39, 1367–1379. doi:10.1002/hbm.23925

Raybuck, J.D., Lattal, K.M., 2014. Bridging the interval: theory and neurobiology of trace conditioning. Behav Processes 101, 103–111. doi:10.1016/j.beproc.2013.08.016

Reichard, R.A., Subramanian, S., Desta, M.T., Sura, T., Becker, M.L., Ghobadi, C.W., Parsley, K.P., Zahm, D.S., 2017. Abundant collateralization of temporal lobe projections to the accumbens, bed nucleus of stria terminalis, central amygdala and lateral septum. Brain Struct Funct 222, 1971–1988. doi:10.1007/s00429-016-1321-y

Reynolds, S.M., Zahm, D.S., 2005. Specificity in the projections of prefrontal and insular cortex to ventral striatopallidum and the extended amygdala. J Neurosci 25, 11757–11767. doi:10.1523/JNEUROSCI.3432-05.2005

Sajdyk, T., Johnson, P., Fitz, S., Shekhar, A., 2008. Chronic inhibition of GABA synthesis in the bed nucleus of the stria terminalis elicits anxiety-like behavior. J Psychopharmacol (Oxford) 22, 633–641. doi:10.1177/0269881107082902

Salas-Wright, C.P., Kagotho, N., Vaughn, M.G., 2014. Mood, anxiety, and personality disorders among first and second-generation immigrants to the United States. Psychiatry Res 220, 1028–1036. doi:10.1016/j.psychres.2014.08.045

Schroijen, M., Fantoni, S., Rivera, C., Vervliet, B., Schruers, K., van den Bergh, O., van Diest, I., 2016. Defensive activation to (un)predictable interoceptive threat: The NPU respiratory threat test (NPUr). Psychophysiology 53, 905–913. doi:10.1111/psyp.12621

Shackman, A.J., Fox, A.S., 2016. Contributions of the central extended amygdala to fear and anxiety. J Neurosci 36, 8050–8063. doi:10.1523/JNEUROSCI.0982-16.2016

Shankman, S.A., Robison-Andrew, E.J., Nelson, B.D., Altman, S.E., Campbell, M.L., 2011. Effects of predictability of shock timing and intensity on aversive responses. Int J Psychophysiol 80, 112–118. doi:10.1016/j.ijpsycho.2011.02.008

Sinnema, H., Majo, M.C., Volker, D., Hoogendoorn, A., Terluin, B., Wensing, M., van Balkom, A., 2015. Effectiveness of a tailored implementation programme to improve recognition, diagnosis and treatment of anxiety and depression in general practice: a cluster randomised controlled trial. Implement Sci 10, 33. doi:10.1186/s13012-015-0210-8

Stein, D.J., Scott, K.M., de Jonge, P., Kessler, R.C., 2017. Epidemiology of anxiety disorders: from surveys to nosology and back. Dialogues Clin Neurosci 19, 127–136.

Sterrenburg, L., Gaszner, B., Boerrigter, J., Santbergen, L., Bramini, M., Roubos, E.W., Peeters, B.W.M.M., Kozicz, T., 2012. Sex-dependent and differential responses to acute restraint stress of corticotropin-releasing factor-producing neurons in the rat paraventricular nucleus, central amygdala, and bed nucleus of the stria terminalis. J Neurosci Res 90, 179–192. doi:10.1002/jnr.22737

Sullivan, G.M., Apergis, J., Bush, D.E.A., Johnson, L.R., Hou, M., Ledoux, J.E., 2004. Lesions in the bed nucleus of the stria terminalis disrupt corticosterone and freezing responses elicited by a contextual but not by a specific cue-conditioned fear stimulus. Neuroscience 128, 7–14. doi:10.1016/j.neuroscience.2004.06.015

Swanson, L., 2003. Brain Maps, Third Edition: Structure of the Rat Brain (Vol 3), 3rd ed. Academic Press.

Takahashi, L.K., 2014. Olfactory systems and neural circuits that modulate predator odor fear. Front Behav Neurosci 8, 72. doi:10.3389/fnbeh.2014.00072

Tipps, M.E., Raybuck, J.D., Buck, K.J., Lattal, K.M., 2014. Delay and trace fear conditioning in C57BL/6 and DBA/2 mice: issues of measurement and performance. Learn Mem 21, 380–393. doi:10.1101/lm.035261.114

Torrisi, S., O'Connell, K., Davis, A., Reynolds, R., Balderston, N., Fudge, J.L., Grillon, C., Ernst, M., 2015. Resting state connectivity of the bed nucleus of the stria terminalis at ultra-high field. Hum Brain Mapp 36, 4076–4088. doi:10.1002/hbm.22899

Verma, D., Tasan, R., Sperk, G., Pape, H.-C., 2018. Neuropeptide Y2 receptors in anteroventral BNST control remote fear memory depending on extinction training. Neurobiol Learn Mem 149, 144–153. doi:10.1016/j.nlm.2018.01.011

Vertes, R.P., 2004. Differential projections of the infralimbic and prelimbic cortex in the rat. Synapse 51, 32–58. doi:10.1002/syn.10279

Waddell, J., Bouton, M.E., Falls, W.A., 2008. Central CRF receptor antagonist a-helical CRF9-41 blocks reinstatement of extinguished fear: the role of the bed nucleus of the stria terminalis. Behav Neurosci 122, 1061–1069. doi:10.1037/a0013136

Waddell, J., Morris, R.W., Bouton, M.E., 2006. Effects of bed nucleus of the stria terminalis lesions on conditioned anxiety: aversive conditioning with long-duration conditional stimuli and reinstatement of extinguished fear. Behav Neurosci 120, 324–336. doi:10.1037/0735-7044.120.2.324

Walker, D.L., Davis, M., 2008. Role of the extended amygdala in short-duration versus sustained fear: a tribute to Dr. Lennart Heimer. Brain Struct Funct 213, 29–42. doi:10.1007/s00429-008-0183-3

Walker, D.L., Miles, L.A., Davis, M., 2009. Selective participation of the bed nucleus of the stria terminalis and CRF in sustained anxiety-like versus phasic fear-like responses. Prog Neuropsychopharmacol Biol Psychiatry 33, 1291–1308. doi:10.1016/j.pnpbp.2009.06.022

Wang, Q., Jin, J., Maren, S., 2016. Renewal of extinguished fear activates ventral hippocampal neurons projecting to the prelimbic and infralimbic cortices in rats. Neurobiol Learn Mem 134 Pt A, 38–43. doi:10.1016/j.nlm.2016.04.002

Weller, K.L., Smith, D.A., 1982. Afferent connections to the bed nucleus of the stria terminalis. Brain Res 232, 255–270. doi:10.1016/0006-8993(82)90272-4

Wittchen, H.-U., 2002. Generalized anxiety disorder: prevalence, burden, and cost to society. Depress Anxiety 16, 162–171. doi:10.1002/da.10065

Xu, H.Y., Liu, Y.J., Xu, M.Y., Zhang, Y.H., Zhang, J.X., Wu, Y.J., 2012. Inactivation of the bed nucleus of the stria terminalis suppresses the innate fear responses of rats induced by the odor of cat urine. Neuroscience 221, 21–27. doi:10.1016/j.neuroscience.2012.06.056

Zelikowsky, M., Bissiere, S., Hast, T.A., Bennett, R.Z., Abdipranoto, A., Vissel, B., Fanselow, M.S., 2013. Prefrontal microcircuit underlies contextual learning after hippocampal loss. Proc Natl Acad Sci U S A 110, 9938–9943. doi:10.1073/pnas.1301691110

Zelikowsky, M., Hui, M., Karigo, T., Choe, A., Yang, B., Blanco, M.R., Beadle, K., Gradinaru, V., Deverman, B.E., Anderson, D.J., 2018. The neuropeptide tac2 controls a distributed

brain state induced by chronic social isolation stress. Cell 173, 1265–1279.e19. doi:10.1016/j.cell.2018.03.037

Zhu, W., Umegaki, H., Suzuki, Y., Miura, H., Iguchi, A., 2001. Involvement of the bed nucleus of the stria terminalis in hippocampal cholinergic system-mediated activation of the hypothalamo--pituitary--adrenocortical axis in rats. Brain Res 916, 101–106.

Zimmerman, J.M., Maren, S., 2011. The bed nucleus of the stria terminalis is required for the expression of contextual but not auditory freezing in rats with basolateral amygdala lesions. Neurobiol Learn Mem 95, 199–205. doi:10.1016/j.nlm.2010.11.002

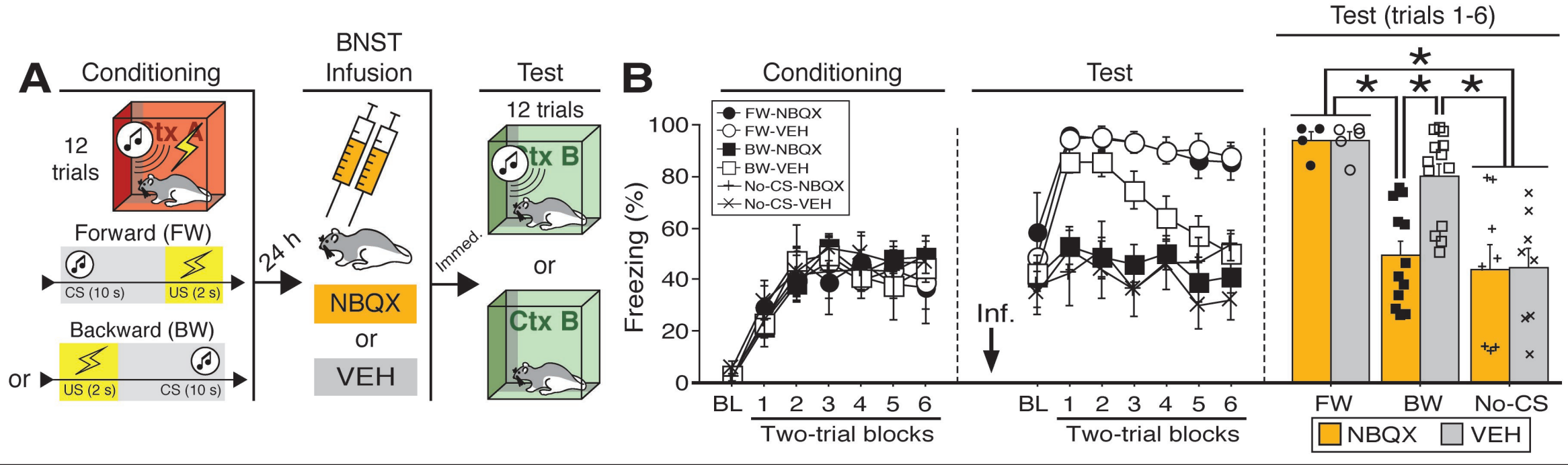
A
Conditioning
12 trials
Ctx A
Forward (FW)
CS (10 s)
US (2 s)
Backward (BW)
or
US (2 s)
CS (10 s)
24 h
BNST Infusion
NBQX
or
VEH
Immed.
Test
12 trials
Ctx B
or
Ctx B
B
Conditioning
Test
FW-NBQX
FW-VEH
BW-NBQX
BW-VEH
No-CS-NBQX
No-CS-VEH
Freezing (%)
100
80
60
40
20
0
BL 1 2 3 4 5 6
Two-trial blocks
Inf.
BL 1 2 3 4 5 6
Two-trial blocks
Test (trials 1-6)
*
*
*
*
FW
BW
No-CS
NBQX
VEH

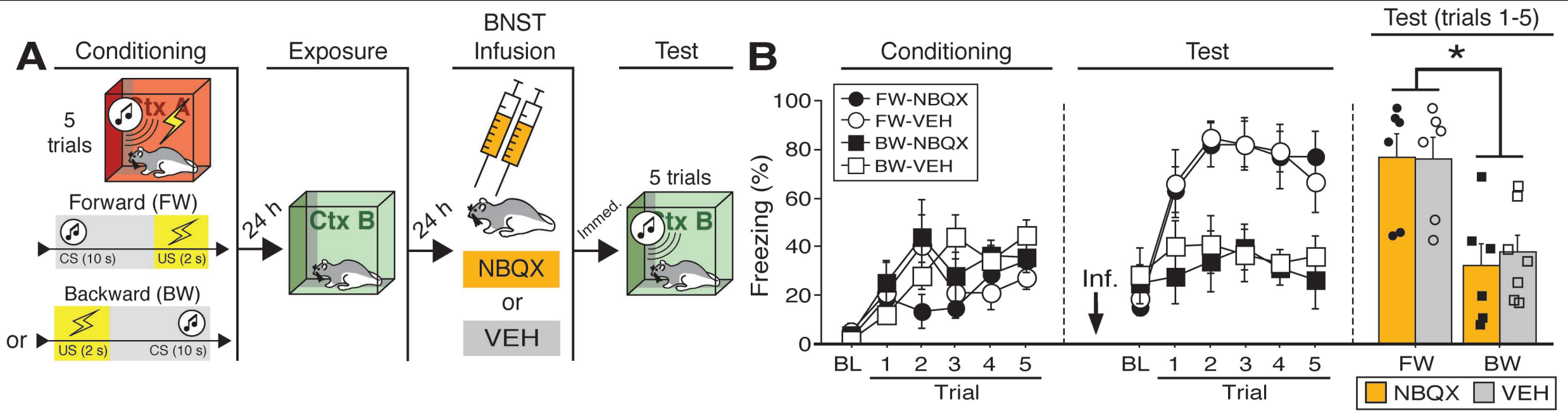
A
Conditioning
Exposure
BNST Infusion
Test
5 trials
Ctx A
Forward (FW)
CS (10 s)
US (2 s)
Backward (BW)
or
US (2 s)
CS (10 s)
24 h
Ctx B
24 h
NBQX
or
VEH
Immed.
5 trials
Ctx B
B
Conditioning
Test
Test (trials 1-5)
FW-NBQX
FW-VEH
BW-NBQX
BW-VEH
Freezing (%)
100
80
60
40
20
0
BL 1 2 3 4 5
Trial
Inf.
BL 1 2 3 4 5
Trial
*
FW
BW
NBQX
VEH

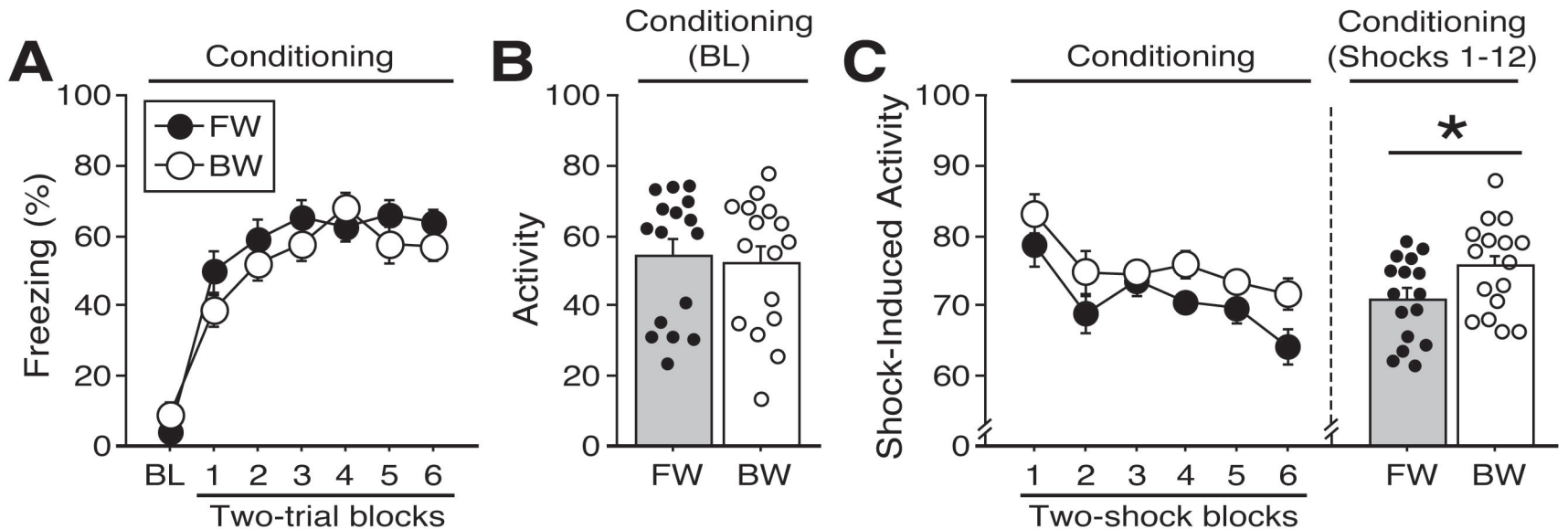
A
Conditioning
FW
BW
Freezing (%)
100
80
60
40
20
0
BL
1
2
3
4
5
6
Two-trial blocks
B
Conditioning
(BL)
Activity
100
80
60
40
20
0
FW
BW
C
Conditioning
Conditioning
(Shocks 1-12)
Shock-Induced Activity
100
90
80
70
60
0
*
1
2
3
4
5
6
Two-shock blocks
FW
BW

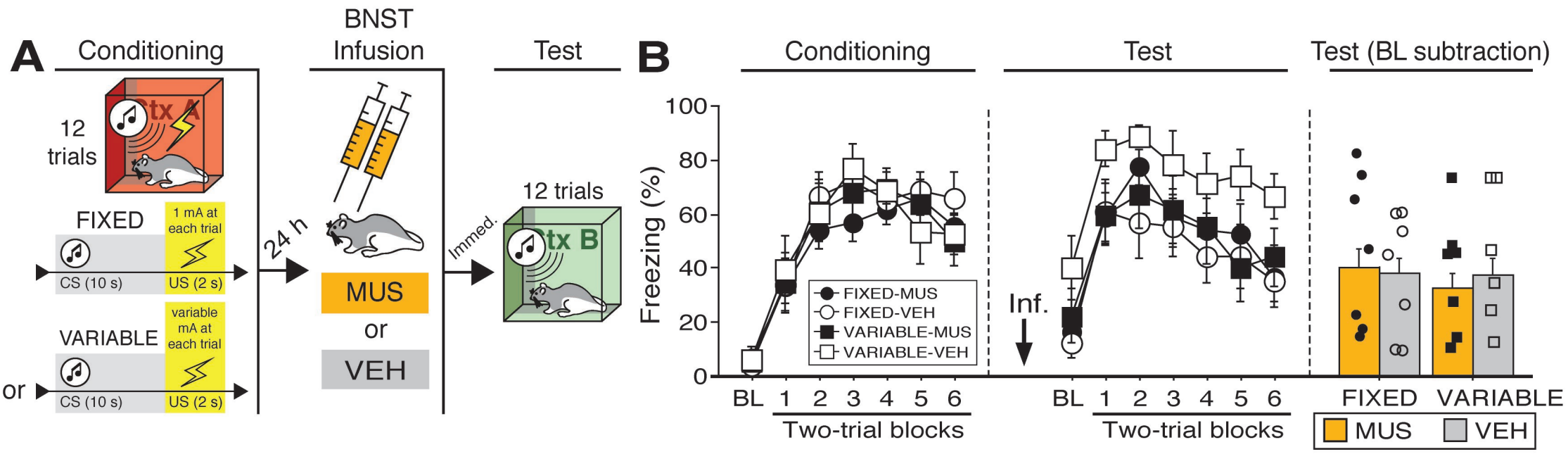
A
Conditioning
BNST Infusion
Test
12 trials
Ctx A
FIXED
1 mA at each trial
CS (10 s)
US (2 s)
VARIABLE
variable mA at each trial
or
24 h
MUS
or
VEH
Immed.
12 trials
Ctx B
B
Conditioning
Test
Test (BL subtraction)
Freezing (%)
100
80
60
40
20
0
FIXED-MUS
FIXED-VEH
VARIABLE-MUS
VARIABLE-VEH
Inf.
BL 1 2 3 4 5 6
Two-trial blocks
FIXED VARIABLE
MUS VEH

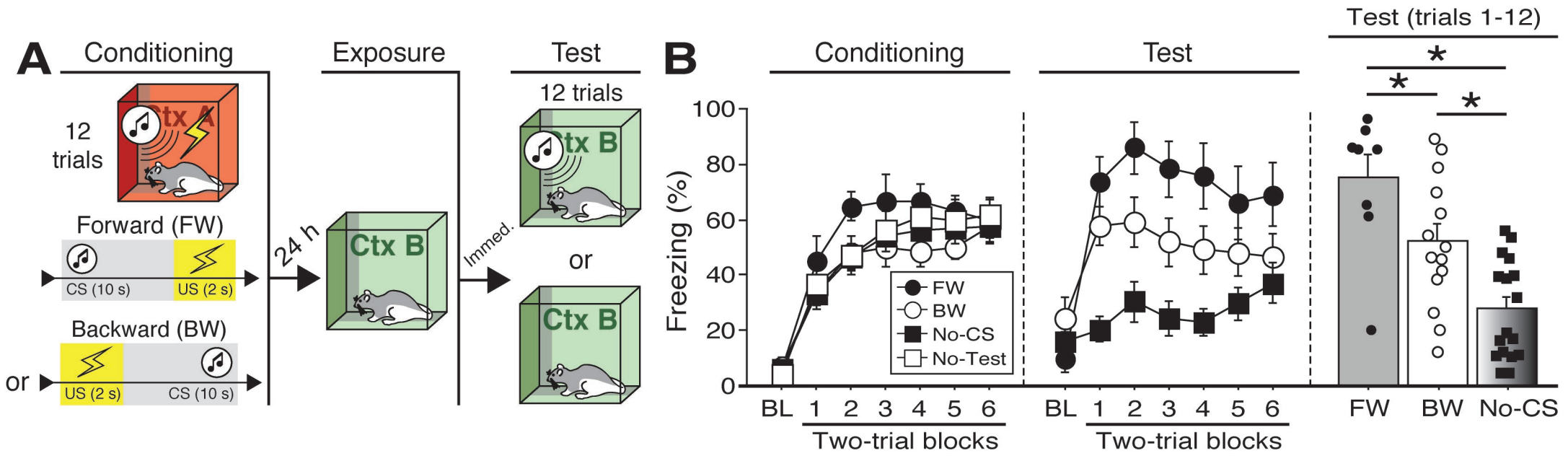
A
Conditioning
Exposure
Test
12 trials
Ctx A
Forward (FW)
CS (10 s)
US (2 s)
Backward (BW)
or
US (2 s)
CS (10 s)
24 h
Ctx B
Immed.
12 trials
Ctx B
or
Ctx B
B
Conditioning
Test
Test (trials 1-12)
Freezing (%)
100
80
60
40
20
0
FW
BW
No-CS
No-Test
BL 1 2 3 4 5 6
Two-trial blocks
BL 1 2 3 4 5 6
Two-trial blocks
FW
BW
No-CS
*
*
*

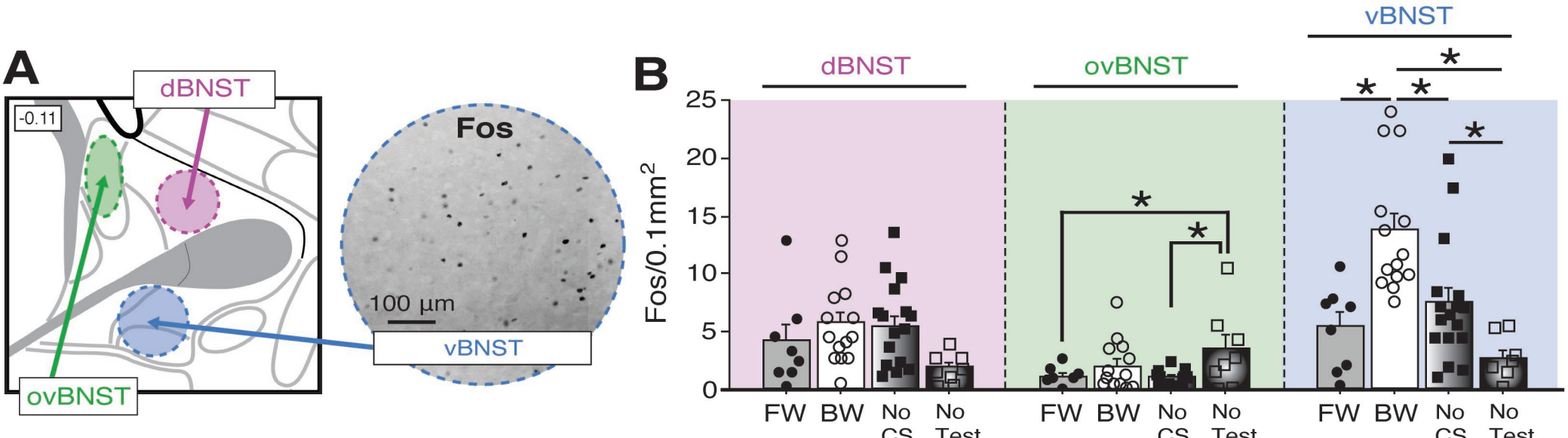
A
dBNST
-0.11
ovBNST
Fos
100 µm
vBNST
B
dBNST
ovBNST
vBNST
Fos/0.1mm²
25
20
15
10
5
0
FW
BW
No CS
No Test
FW
BW
No CS
No Test
FW
BW
No CS
No Test

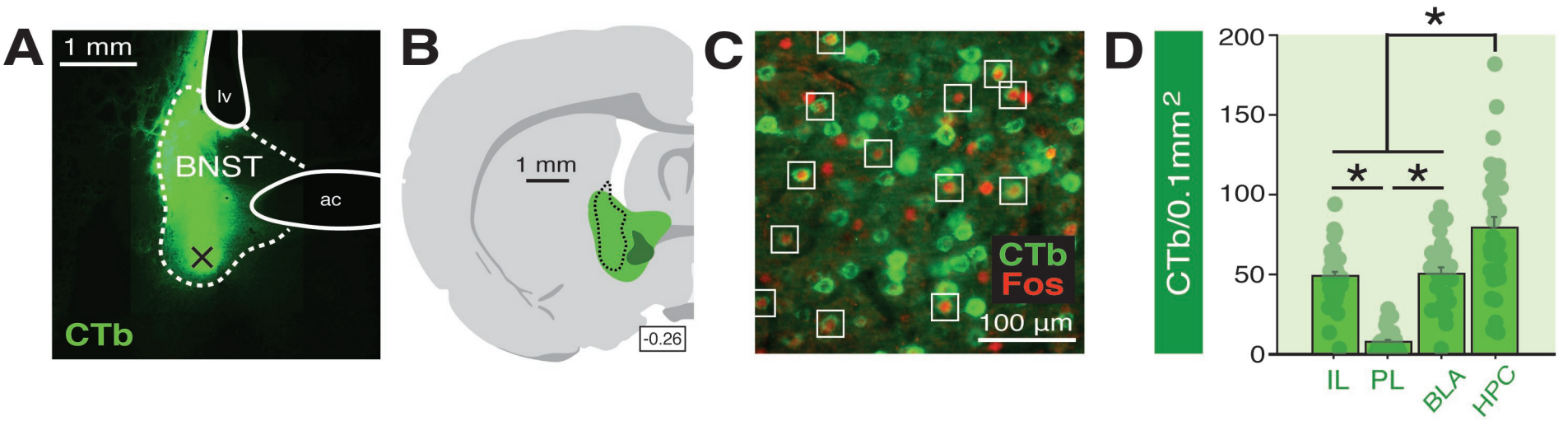
A
1 mm
lv
BNST
ac
CTb
B
1 mm
-0.26
C
CTb
Fos
100 µm
D
CTb/0.1mm2
200
150
100
50
0
*
*
*
IL
PL
BLA
HPC

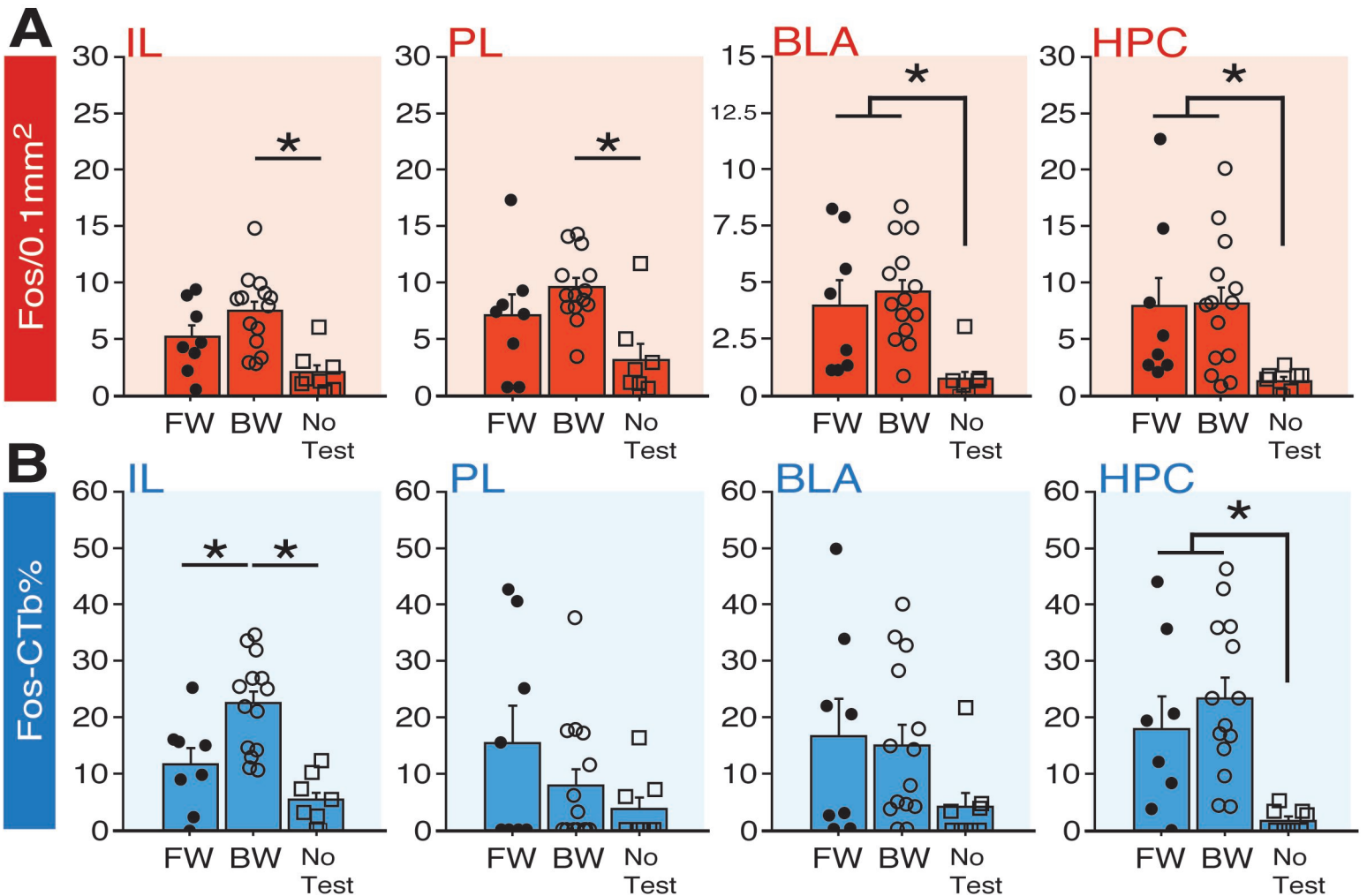
A
IL
PL
BLA
HPC
Fos/0.1mm2
30
25
20
15
10
5
0
12.5
7.5
2.5
*
FW
BW
No Test
B
Fos-CTb%
60
50
40
30
20
10
0

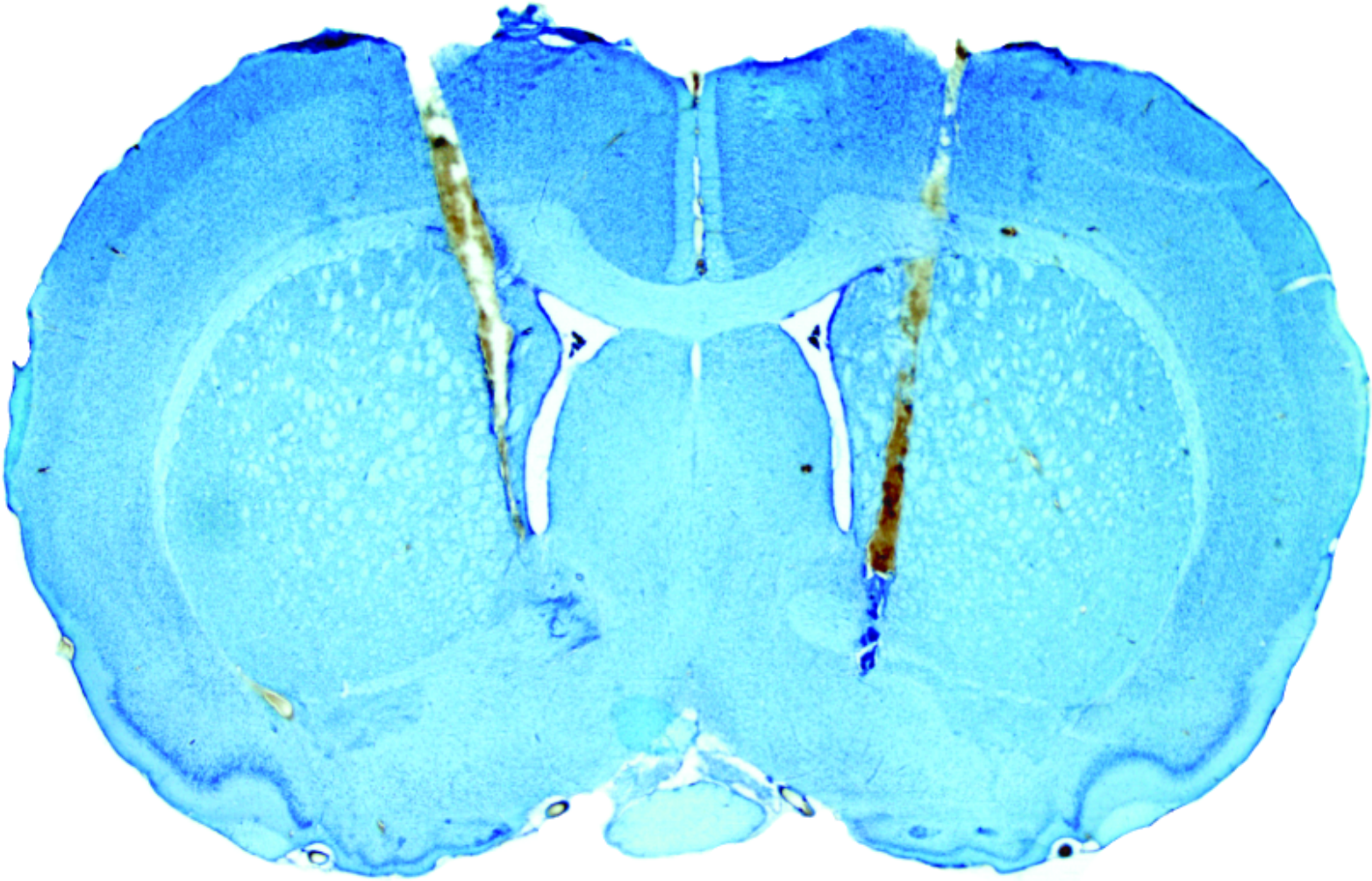

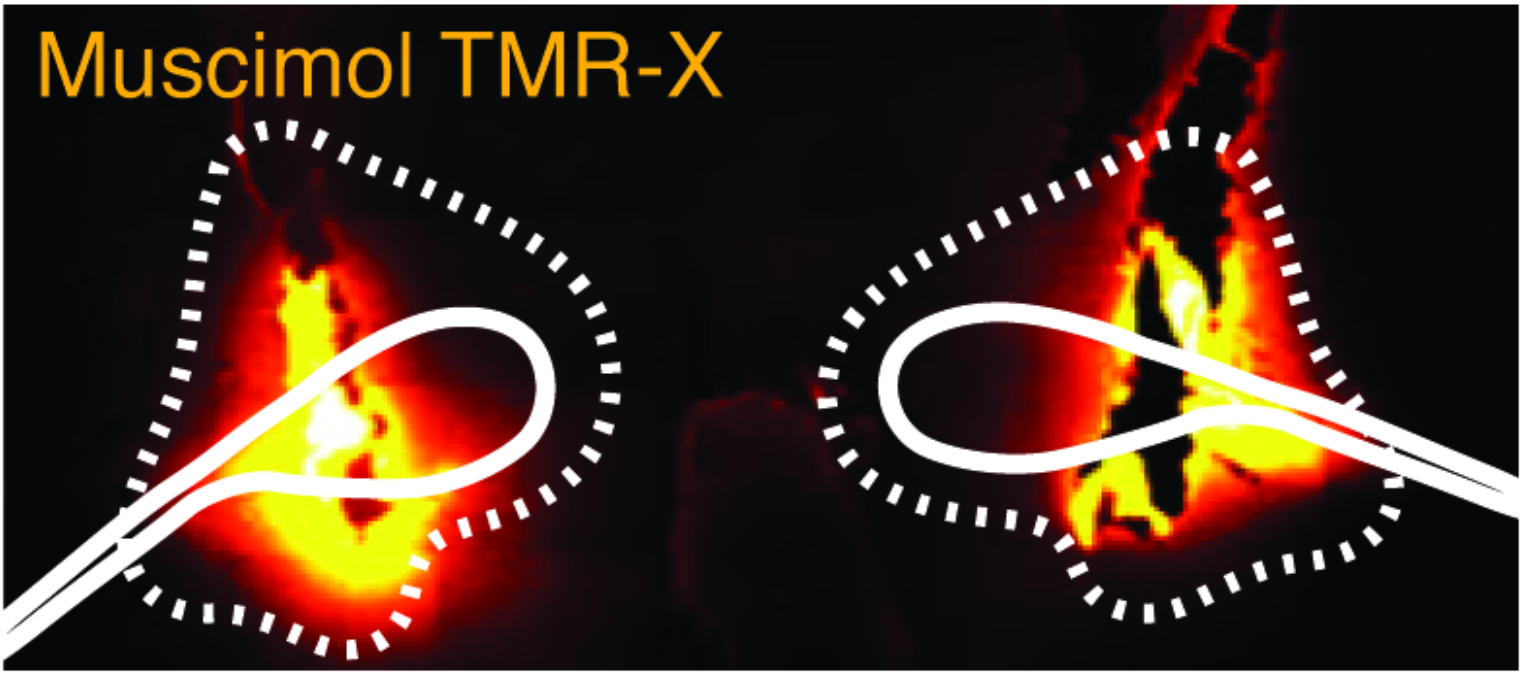
Muscimol TMR-X

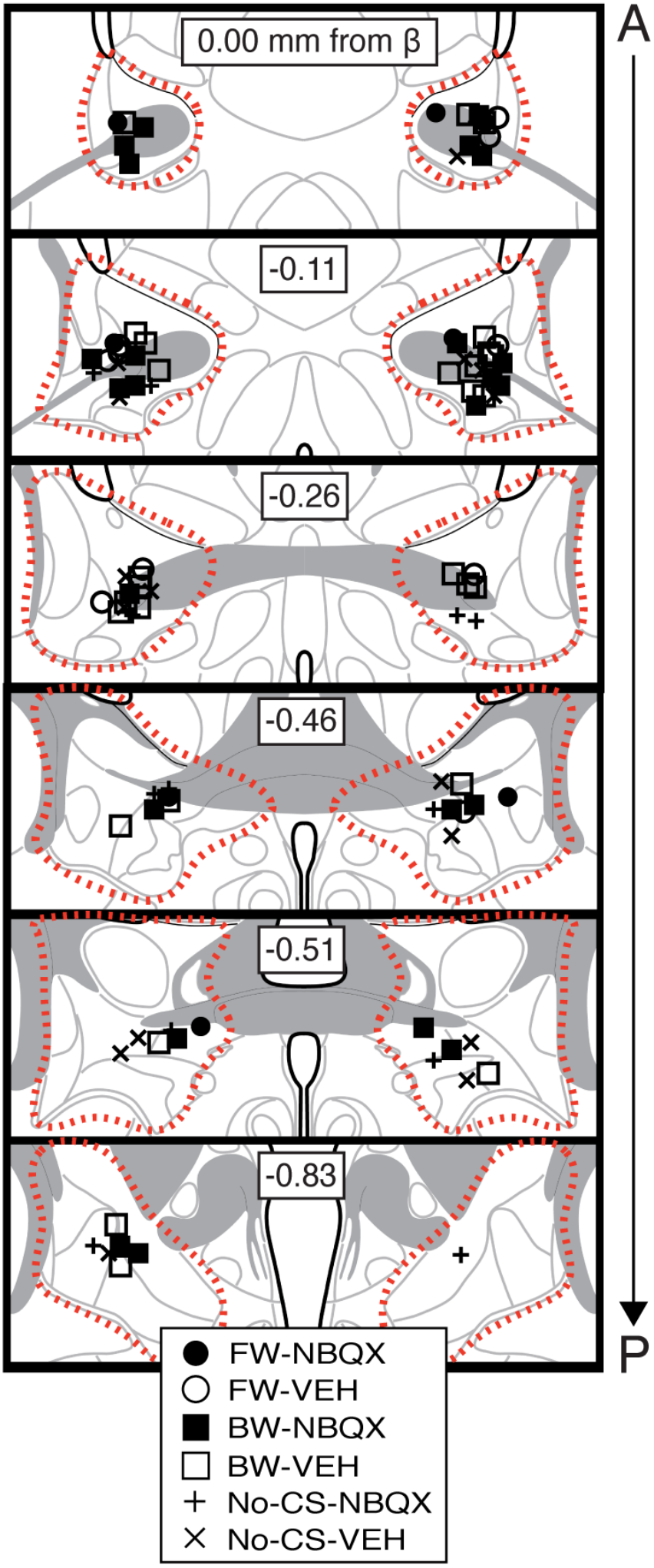
0.00 mm from β
-0.11
-0.26
-0.46
-0.51
-0.83
A
P
FW-NBQX
FW-VEH
BW-NBQX
BW-VEH
No-CS-NBQX
No-CS-VEH

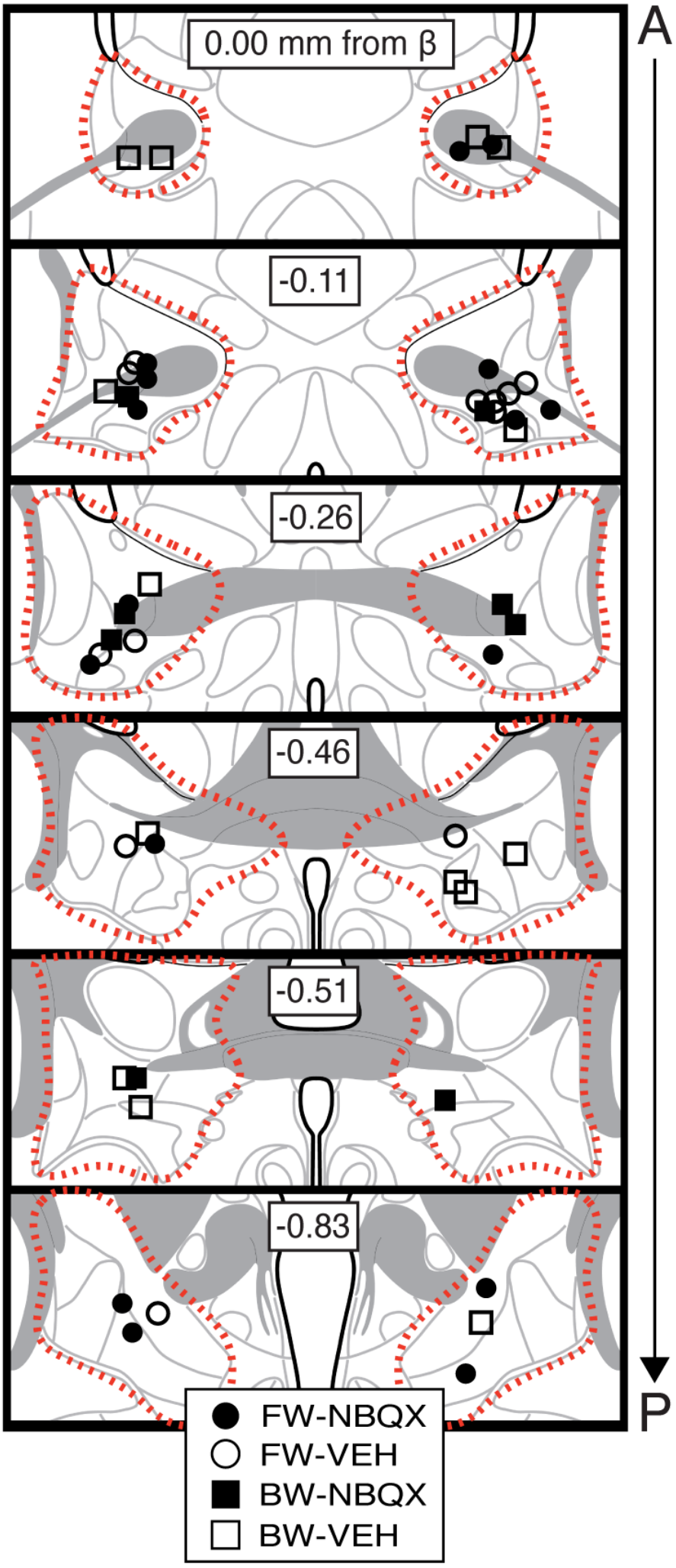
0.00 mm from β
-0.11
-0.26
-0.46
-0.51
-0.83
A
P
FW-NBQX
FW-VEH
BW-NBQX
BW-VEH

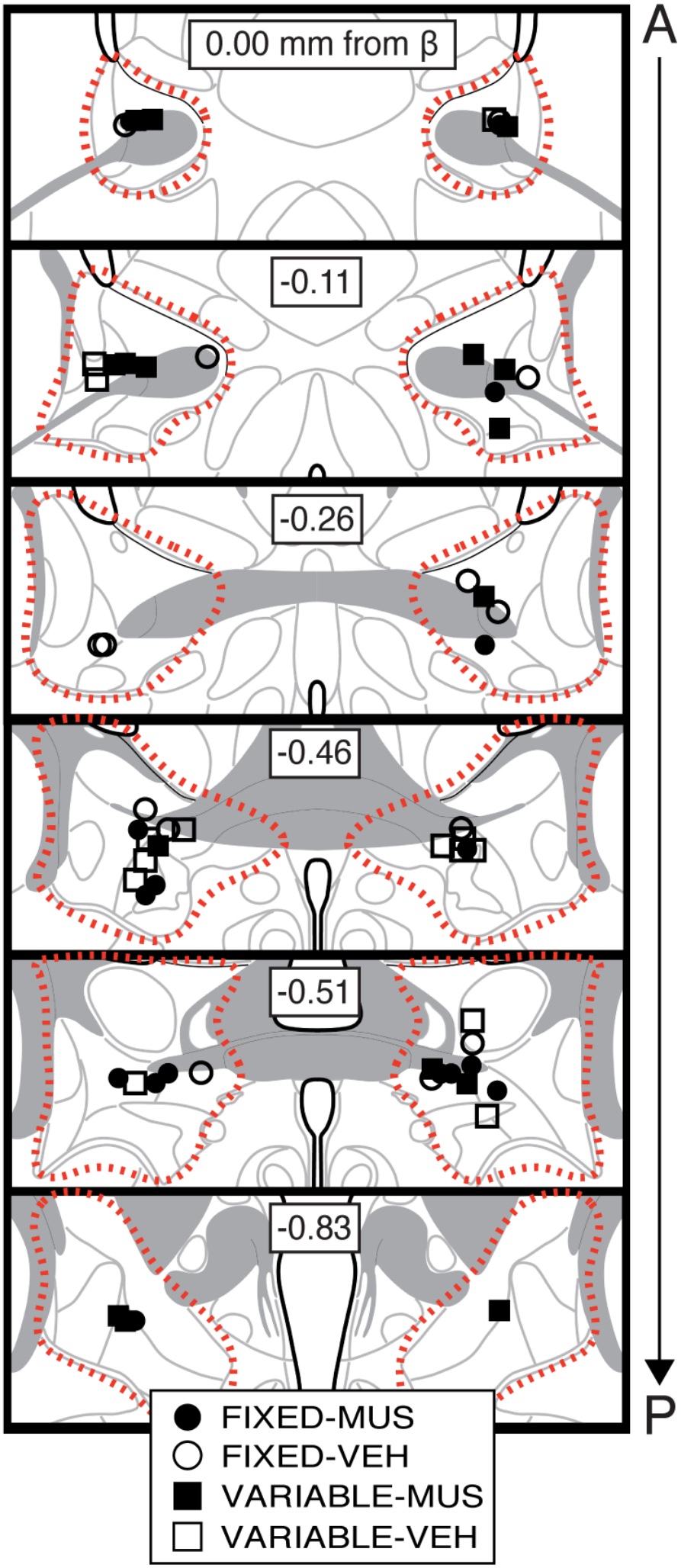
0.00 mm from β
-0.11
-0.26
-0.46
-0.51
-0.83
A
P
FIXED-MUS
FIXED-VEH
VARIABLE-MUS
VARIABLE-VEH

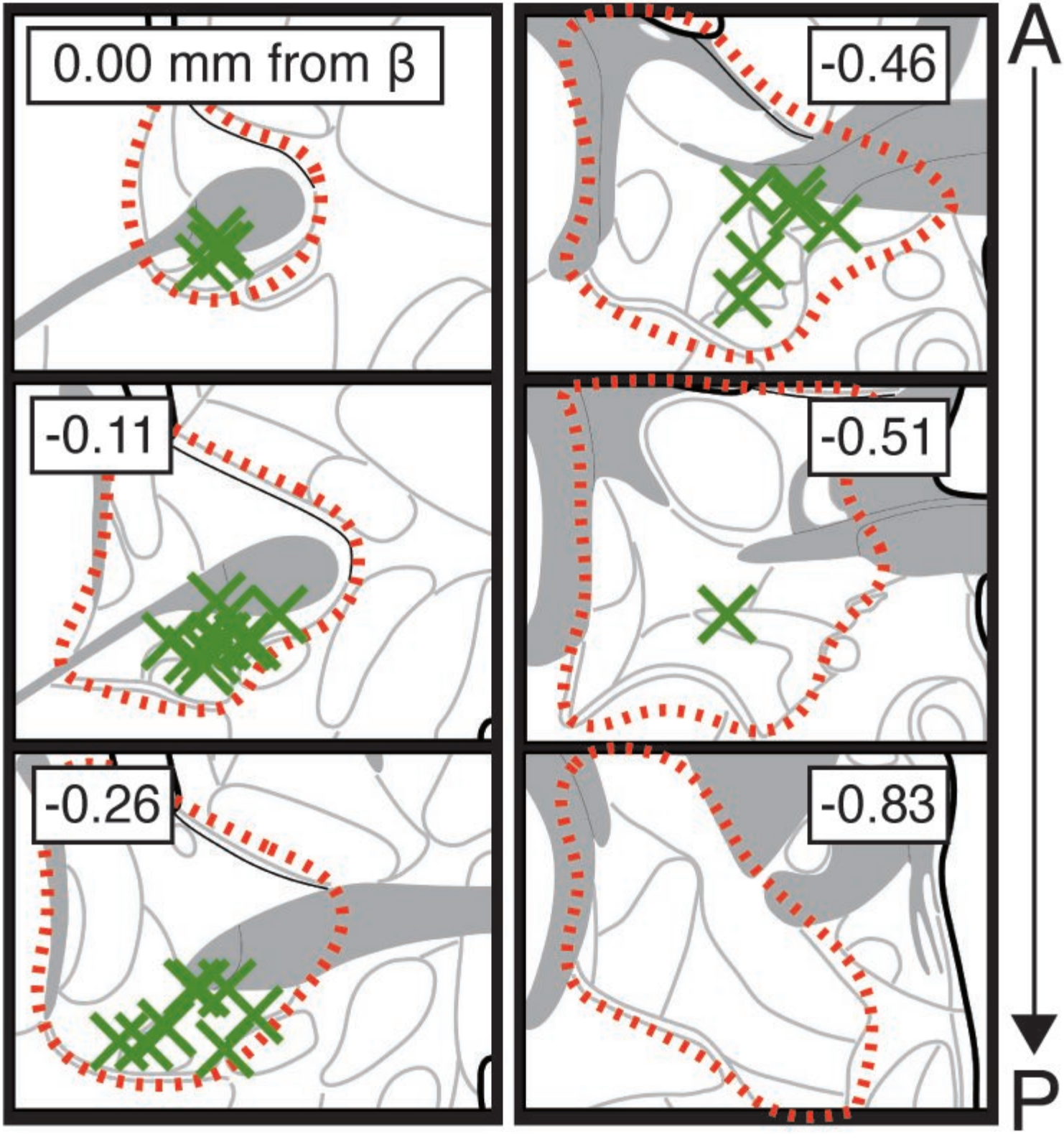
0.00 mm from β
-0.11
-0.26
-0.46
-0.51
-0.83
A
P